Novel use of Advanced Scatterometer (ASCAT) for forest fire monitoring

MSc. Thesis

Emma Blanken

Delft University of Technology

TU Delft

Novel use of Advanced Scatterometer (ASCAT) for forest fire monitoring

by

Emma Blanken

to obtain the degree of Master of Science
at the Delft University of Technology,
to be defended publicly on Tuesday April 18, 2023 at 13.30h.

Student number:	4453808	
Thesis committee:	Prof. dr. ir. S. Steele-Dunne	TU Delft
	Dr. S. L. M. Lhermitte	TU Delft, KU Leuven
	Dr. ir. P. López-Dekker	TU Delft

Cover: Eucalyptus trees with epicormic resprouting 4 months after forest fires. Picture was taken in Madeira. Source: GerritR, CC BY-SA 4.0, via Wikimedia Commons

Style: TU Delft Report Style, with modifications by Daan Zwaneveld

An electronic version of this thesis is available at http://repository.tudelft.nl/.

TU Delft

Summary

Fire both shapes and destroys forests. Forest fires are therefore essential to ecological processes and vegetation as we know them. With climate change, forest fires are expected to increase in severity and frequency. To maintain the functioning of the forests, it is important to understand the vegetation response to and recovery from forest fires. Within this field of study, remote sensing techniques are common, and optical indices such as the NDVI are most prevalent.

With recent developments, the ASCAT variables slope and curvature have become of increasing interest in structural vegetation monitoring. These variables are a second-order Taylor polynomial's first and second derivatives used to normalise the ASCAT backscatter-incidence angle relationship. This study explored the possibility to use these novel variables in forest fire research. The focus was to discover to what extent the variables responded to a major forest fire.

To do so, grid points affected during the 2009 Australian Black Saturday Fires are compared to unaffected control grid points utilizing Z-scores. These control grid points have been selected based on time series similarity in the two years before the fire. Time series from 2007 to 2021 are used to investigate fire impact and recovery. The ASCAT variables are compared to a similar NDVI time series to aid in interpreting the results.

The findings show that both slope and curvature are sensitive to the major forest fire. Both variables show an impact shortly after the fire, which can be explained by the loss of scattering elements in the vegetation due to the fire. In the following years, there is a notable recovery which can be explained by the vegetation regrowth forming new scatterers. The NDVI showed similar behaviour but the recovery was differently timed, suggesting that the signal recovery is driven by something else or that the regrowth of leaves is different from the regrowth of the structural elements that the ASCAT variables represent.

The results help in understanding the ASCAT variables and their interpretation in terms of vegetation scatterers. Especially for the curvature, the clear change in signal deflects the discussion of whether the variable has information potential. Nevertheless, for the ASCAT variables to be applicable in forest fire research, they need to be better understood and additional research is necessary. Suggestions are for example a ground validation study or a global forest fire study, which would suit the coarse resolution of the ASCAT variables better and improve the understanding of the interaction between forest fires and the variables.

Although using the ASCAT variable for forest fire research is in its infancy, the results about its suitability are promising, both for ASCAT product development, as well as for the forest fire research field. Exploring the possibilities further is worthwhile, especially considering the fact that the slope and curvature time series cover a long continuous period starting as early as 1991. This long time series makes the ASCAT variables suitable for long-term forest fire monitoring, and the daily nature of the data might also make them interesting for short-term monitoring.

Fanning the Flames

The sky is ablaze.

Waves of dirty yellows
wash over the ground,
as crimson smoke licks
barren clouds that loiter
jeeringly overhead.

Fuel litters the floor,
its perilous potential scattered
absently across the detritus;
the cost of its appearance
obscured by the multitude
of our transactions.

Silhouettes flicker across the canopy,
their panicked hosts seeking refuge
in havens that we have long since razed.

We branded these trees in all of our names,
Forgetting the forest until it burnt in the flames.

Sam Illingworth[1], 2020

[1]In 2019, I attended a lecture by Sam Illingworth, and his approach to Science Communication stuck with me ever since. On his website 'The Poetry Of Science', he writes poems about recent academic research to develop the dialogue between scientists and non-scientists. This poem is based on research about how logging in the Australian Eucalyptus forest worsened the 2020 'Black Summer' forest fires, which were even more catastrophic than the Black Saturday fires that are the subject of this study.

Preface

If you had told me 8 years ago my graduation project would have something to do with microwaves, I would have thought that I had made a questionable switch to culinary school with an even more questionable specialization in microwaves - the thing that warms your bowl, but not your dish. But here we are, and I am proud to present my thesis that involves microwaves, but fortunately, is way more than that.

Nearing the end of my time as a student, writing a joke about microwaves makes me realise how much I have learned and how far I have come. Studying was not always easy, and the last few years were different from what I had imagined them. 'Stressed' is a word that will always be a part of me, but I learned to understand it. However, in between the stress, the unreasonably long study days during my bachelor's, and the more structured but still demanding study days in my master's, I also had a lot of fun and made unforgettable memories.

I want to thank my supervisors Susan and Stef. Thank you for your boundless patience and understanding. I am very grateful for your help; from explaining the ASCAT variables to me for the thousandth time to forcing me to stop coming up with new analyses and just start writing. Most importantly, thank you for instilling confidence in my own research. If it's up to me, you can keep the weekly meeting on your agenda forever to appear busy for an hour and do some work in silence. I also would like to thank Paco for joining the committee and believing in my thesis.

As you may know, I spend a lot of time on Science Communication, and although I did not finish the program, I gained a lot from it. I want to thank the PDP bunch - you are inspiring people and sticking post-its on a whiteboard wouldn't be as fun without you. To everyone who read my thesis, thank you for the feedback, it was invaluable. To my AES and GRS study friends - Jeanne, Mo, Anna Lisa, Marije, Daan, and Goof - thank you for keeping me sane during the projects and enlightening my days with coffee breaks more often than necessary. Daan, thank you for being my self-proclaimed 'ghost-supervisor' and I am sorry that we will never agree on how a conclusion should look. Goof, thank you for pushing me to be social during times of need. To my roommates, Esmay and Daiva, thank you for everything - from living room dance parties to making the AVS a home. To Laurence, Gitte, Sophie W, Sophie T and others: thanks for the distractions, the advice and the encouragement over the past years. To Mom, Dad, Duco and Thijs: Little Emma isn't that little anymore, thank you for getting her here. And lastly, Rik, you are simply amazing, I couldn't even start to thank you for everything.

Enjoy my thesis, and hopefully, you will learn a thing or two about how the now probably mysterious 'ASCAT variables' and forest fires are related.

Emma Blanken
Leiden, March 2023

Contents

1

Introduction

Fire both shapes and destroys forests. Forest fires are essential to ecological processes and vegetation as we know them, and without them, the world would look completely different (Bond et al., 2005). This is especially true for eucalyptus forests in Australia, which are known for their tolerance to and reliance on fire (Adams & Attiwill, 2011; Gill, 1981). However, even the typically fire-tolerant eucalyptus forests are under pressure with increasing fire frequency and severity due to climate change (Fairman et al., 2016). With this increasing pressure, the structure, composition and ecological functioning of these forests are in danger. Therefore, it is of increasing importance to understand how these forests react to and recover from forest fires in an effort to maintain them, in terms of structure and ecosystem functioning.

Remote Sensing techniques are a time- and cost-effective way to monitor fire effects, both in terms of impact and post-fire recovery of the vegetation at the landscape level (for extensive reviews see Chuvieco et al. (2020), Pérez-Cabello et al. (2021), and M. A. Tanase et al. (2015)). A fire disturbance affects and alters the vegetation and these changes can be measured by remote sensing techniques. Examples of what might be measured are a decrease in photosynthetic activity, shifts in vegetation phenology, structural changes as well as changes in the functioning of the landscape (João et al., 2018). For the monitoring, analysing and mapping of temporal and spatial vegetation changes as a result of forest fires, multi-spectral optical satellite imagery is most commonly used. Especially the use of the Normalized Difference Vegetation Index (NDVI) and the Normalized Burn Ratio (NBR) has been widespread. These vegetation indices provide a good proxy for both mapping burn severity levels as well as for vegetative regrowth, due to their sensitivity to chlorophyll concentration, canopy greenness, vigour (NDVI) and leaf moisture (NBR).

However, these spectral vegetation indices (VI) tend to saturate over dense vegetation (Pérez-Cabello et al., 2021) and are less accurate in change detection over high fire severities (M. A. Tanase et al., 2015). These spectral VI's respond to canopy cover rather than vegetation structure, as a result of which they reach full spectral recovery rather quickly after a fire when leaves start to regrow. Even at sites which have been burned by high severity, the young regrowth might quickly show a similar NDVI signal as the previous mature canopy (Karna et al., 2020; M. Tanase et al., 2011). However, forests may need decades to reach a mature stage in which they can provide the same ecological functions as before the fire (Benyon & Lane, 2013; M. Tanase et al., 2011), and the quickly saturated spectral VI's provide little value in monitoring this long-term recovery. Alongside the saturation, the spectral VI's are also sensitive to cloud cover and are unable to measure structural changes caused by a disturbance. These structural changes might be more indicative of a forest's return to pre-fire ecological functioning than the 'greenness' or canopy cover is. This is especially the case for Eucalyptus forests which even after high fire severities quickly recover via epicormic resprouting; recovering a green canopy but with a drastically altered structure (Karna et al., 2020).

To measure the structural effects of forest fires, sensors that respond to scattering elements rather than spectral signals may offer a solution. Active sensors are used as they are known to be sensitive to vegetation structure, and indeed signals complementary to the spectral VI's were found. M. Tanase et al. (2010) found PALSAR L-band SAR to be able to distinguish between different fire severities in several forest types, as an increasing fire severity reduced the scatterers in the canopy layer, increasing the dominance of ground scattering. With the same PALSAR L-band SAR, M. Tanase et al. (2011) found sensitivity to forest regrowth where several growth stages could be distinguished, of which only few could be identified from NDVI measurements. Fernandez-Carrillo et al. (2019) once again used L-band SAR to measure short-term recovery from prescribed fires in Eucalyptus forests. Additionally, Polychronaki (2014) used ERS backscatter coefficients in combination with NDVI and found that the ERS backscatter coefficients were especially useful in the recovery of dense forests, where the NDVI quickly reached saturation. LiDAR has also shown structural changes of the canopy seven years after a Eucalyptus forest fire when the forest was already spectrally recovered (Karna et al., 2020). Many more examples exist of LiDAR and both active and passive microwaves' suitability for forest fire impact and recovery assessment.

With recent development in the TU Wien Soil Moisture Retrieval (TUW SMR) algorithm, a new possibility emerges to use active microwave measurements in forest fire research. The TUW SMR retrieves soil moisture from ERS/ASCAT backscatter. The algorithm is based on the relationship between backscatter σ and incidence angle θ. To normalise this relationship to a common reference angle θ_r, a second-order polynomial is used. The first and second-order derivatives of this polynomial are not only used to normalise the backscatter measurements, but also to correct for vegetation (Hahn et al., 2017).

To utilise this second-order polynomial, the first- and second-order derivatives (slope σ' and curvature σ'', respectively) need to be determined. To do so, the fore-, mid- and aft-beam of the ERS instrument were initially used to determine a local slope. From this local slope, the slope and curvature can be determined. However, local slope values are noisy and many measurements are needed to obtain a robust result. Therefore, seasonalities of the local slope are used to determine σ' and σ'', and consequently, soil moisture results were calculated assuming the vegetation has no inter-annual differences. With the addition of another set of fore-, mid- and aft-beams to the newer ASCAT instruments, data density went up, and slope and curvature could be determined dynamically, rather than as a seasonality (Melzer, 2013). This improved the TUW SMR (Hahn et al., 2017; Steele-Dunne et al., 2021), but also created the possibility to use σ' and σ'' not only for backscatter normalisation and vegetation correction but as self-contained data sources for vegetation research (Steele-Dunne et al., 2019).

Similar to the previously mentioned SAR, the slope and curvature respond to vegetation scatterers and wet above-ground biomass. Slope and curvature describe the backscatter behaviour as a function of the incidence angle. When there is bare soil, surface scattering is the dominant scattering signal, and only little signal is scattered back at high incidence angle. When there is more vegetation present, volume and multiple scattering become more prevalent, and parts of the signal are scattered back even at high incidence angles. This is described by a less steep slope σ'. This can also be described as the backscatter becoming increasingly incidence angle independent.

Initially, the slope was considered a proxy of vegetation density to account for the effects of vegetation attenuation on soil moisture retrieval. Currently, the slope is used to describe the wet above-ground biomass of the vegetation and its scattering mechanisms. It is thus not directly related to vegetation greenness for which for example the NDVI is a proxy. A high slope (close to zero, less steep) describes scattering that is largely incidence angle independent, thus where volume and multiple scattering are dominant. Volume and multiple scattering are related to, but not necessarily the same as, high vegetation density. Curvature is less well understood but has been found to be influenced by vegetation structure and phenology. Steele-Dunne et al. (2019) established that curvature 'contains some information about vegetation independent of slope', for

example in the case of highly vertical structures leading to high σ and high θ. It is therefore at least related to the verticality of the vegetation structure.

Both slope σ' and curvature σ'' are novel variables for vegetation research. Interpretations, therefore, remain subject to change. With the current understanding and for the sake of this study, they are understood in terms of scattering mechanisms. A change in slope and curvature, therefore, represents a change in scattering elements and scattering mechanism. With these properties, we hypothesised that slope σ' and curvature σ" (referred to as the ASCAT variables) should be able to measure impact and recovery after forest fires. Fire is known to remove scatters from the forest, and over time the scatterers will increase again as the forest regrows. Not only the number of scatterers will have changed due to a forest fire, but also the size, shape, distribution and the water content.

This study tries to create a qualitative understanding of whether the ASCAT variables are sensitive to forest fire effects in terms of impact and recovery following a major forest fire. To interpret the results, the ASCAT variables are compared to the commonly used post-forest fire index NDVI. The study thus sets out to answer the following questions:

1. To what extent do the ASCAT variables show an impact in response to forest fire?
2. To what extent do the ASCAT variables show a recovery following forest fire?
3. To what extent do the ASCAT variable responses relate to or complement NDVI forest fire analysis?

2

Study Area, Data & Methods

In this study, we investigate the response of the ASCAT variables to a major forest fire. To do so, we compare time series of affected ASCAT grid points to time series of unaffected ASCAT grid points by means of a Z-score. To interpret the results it is important to understand the anatomy of the forest fire as well as the vegetation response, which are discussed in Section 2.1. The ASCAT variable Z-scores are compared to NDVI Z-scores, which are resampled to the same spatial resolution. The NDVI Z-scores acts as a benchmark for the ASCAT variables, but it also used to investigate the complementarity of the three different variables. Additional to the comparison between the different variables, the Z-score time series are also analysed in terms of fire severity. Fire severity is directly related to impact and also influences the vegetation response in recovery (João et al., 2018). In Section 2.2, the different data sources as well as their pre-processing to the same spatial resolution are discussed. In Section 2.3, the processing of the raw variable time series to Z-scores is discussed, as well as how these results are interpreted.

2.1. Study Area

On Saturday 7 February 2009, a forest fire burned over 450,000 ha in Victoria, Australia. The wildfire, infamously known as the 'Black Saturday' fires, took 173 lives and destroyed more than 2000 homes (Cruz et al., 2012). Such a catastrophic wildfire was the result of a 12-year drought (known as the Millenium Drought) causing extremely dry fuel loads and extreme fire weather in the preceeding two weeks, such as high temperatures and strong hot winds. The most significant fire in the Black Saturday fires was the Killmore-Murrindi complex, which burnt for three weeks, but in which most of the damage was done already in the first 12 hours (Cruz et al., 2012).

The area in which the Killmore-Murrindi complex took place encompasses a large range of topography, fuel loads and vegetation types (Benyon & Lane, 2013; Cruz et al., 2012). Those spatial differences lead to a highly spatially diverse fire severity, where some areas were burned with low severities, barely affecting the vegetation understorey, and other areas burned with high severities and experienced complete canopy crown burn (Department of Environment, Land, Water and Planning, 2018b). The fire's extent and severity are shown in Figure 2.1. The fire severity is a scale from Fire Severity 1 (FS1) up to 5 (FS5), where FS1 represent the most fire damage and is referred to as a high fire severity. In an FS1 fire, both the understory and the upper canopy are consumed. FS5 represents a fire with the least damage done, where only parts of the understory are affected. This is commonly referred to as low fire severity. Moderate fire severity is represented by FS3, where the upper canopy is affected but not consumed. More on the fire severity will be explained in Section 2.2.3.

The region in which the Killmore-Murrindi complex took place has a temperate climate with a mild (and drier) summer. The annual rainfall is between 800-1200mm and increases from west to east. In Winter (June, July & August) the average monthly minimum temperature is 4° C, and the

average monthly maximum is 9° C. The Summer (December, January & February) has a minimum temperature of 12° C and the mean monthly maximum is up to 23° C (Bureau of Meteorology, 2016). The area falls within the foothills of the Great Dividing Range, and therefore is hilly and mountainous, containing numerous, steep, gullies, which are wetter than the surrounding hills (Leonard et al., 2014).

2.1.1. Vegetation

The extent of the Killmore-Murindi fire complex covers mostly natural forests, including several national parks and state forests. Within this area, the major vegetation classes as mapped by the Department of Environment, Land, Water and Planning (2018a) are 'Dry Forest', 'Wet and Damp Forest' and patches of 'Cool Temperate Rainforest' within the steep gullies. However, within this study, the focus is on the first two (also see 2.2.4, Figure 2.1). Both have a dominant Eucalyptus overstorey, which is known for its resilience to both drought and fire. Eucalyptus trees hold their leaves perpendicular to the ground, allowing light to penetrate to the understorey (Heath et al., 2016). Spatially, Dry Forest often transitions into Damp Forest which transitions into Wet Forest with increasing rainfall and moisture (Gullan, 2008a), but in this study, Wet and Damp Forest are grouped together and referred to as Wet Forest, as they are deemed to be the same major vegetation class in the Department of Environment, Land, Water and Planning (2018a) dataset as well. Examples of the appearance of the forest types are shown in Figure 2.2.

- **Dry Forest**: also known as dry sclerophyll forest, open forest or 'Herb rich foothill forest' (Bennett et al., 2016; Karna et al., 2020). It is the largest class within the study area and covers most of the western part of the fire complex, as well as the lower elevation areas in the east. It contains a mix of fire-tolerant eucalyptus species as overstory such as *E. Radiata*, *E. Obliqua*, *E. Dives* (Bennett et al., 2016; Karna et al., 2020; Leonard et al., 2014). This class is characterized by crooked, spread trees up to 30m in height and a projective foliage cover of 30-70%. The understorey is normally sparse sclerophyllous shrubs, and a species-rich ground cover of grasses, ferns and small herbs (Gullan, 2008b; Karna et al., 2020).
- **Wet and Damp Forest**, also known as wet sclerophyll forest, (damp sclerophyll forest) and closed cover forest. In addition to the tree species in the Dry Forest, the wet forest contains 'Ash type' eucalyptus trees such as *E. Regnans* and *E. Delegatenis* (Benyon & Lane, 2013). The wet forest mostly occurs in the East of the fire complex, where rainfall is higher, or in the higher elevation areas surrounding Mount Disappointment in the West (Benyon & Lane, 2013; Leonard et al., 2014). The overstorey eucalyptus trees reach heights of 40-75m depending on how wet the area is, and typically grow quickly, resulting in straight, tall trees (Gullan, 2008c). The Wet Forest has denser foliage than the Dry Forest. There is a dense understorey of shrubs, climbers, non-eucalypt tree species and tree ferns. The ground layer is generally sparsely vegetated, but the vegetation that is present is dominantly ferns (Leonard et al., 2014), there are also some small herbs and coarse grasses (Gullan, 2008c). The Wet Forest has a clearer canopy layering than the Dry Forest. The Wet Forest is also characterised by a large amount of litter on the forest floor, which creates high fuel loads. In general, these fuel loads are typically wet and therefore do not burn. In dry and hot extreme conditions, however, the fuel switches from being too wet to burn, to being extremely flammable. Therefore, wet eucalyptus forest is more likely than Dry Forest to experience high-intensity fires (Leonard et al., 2014).

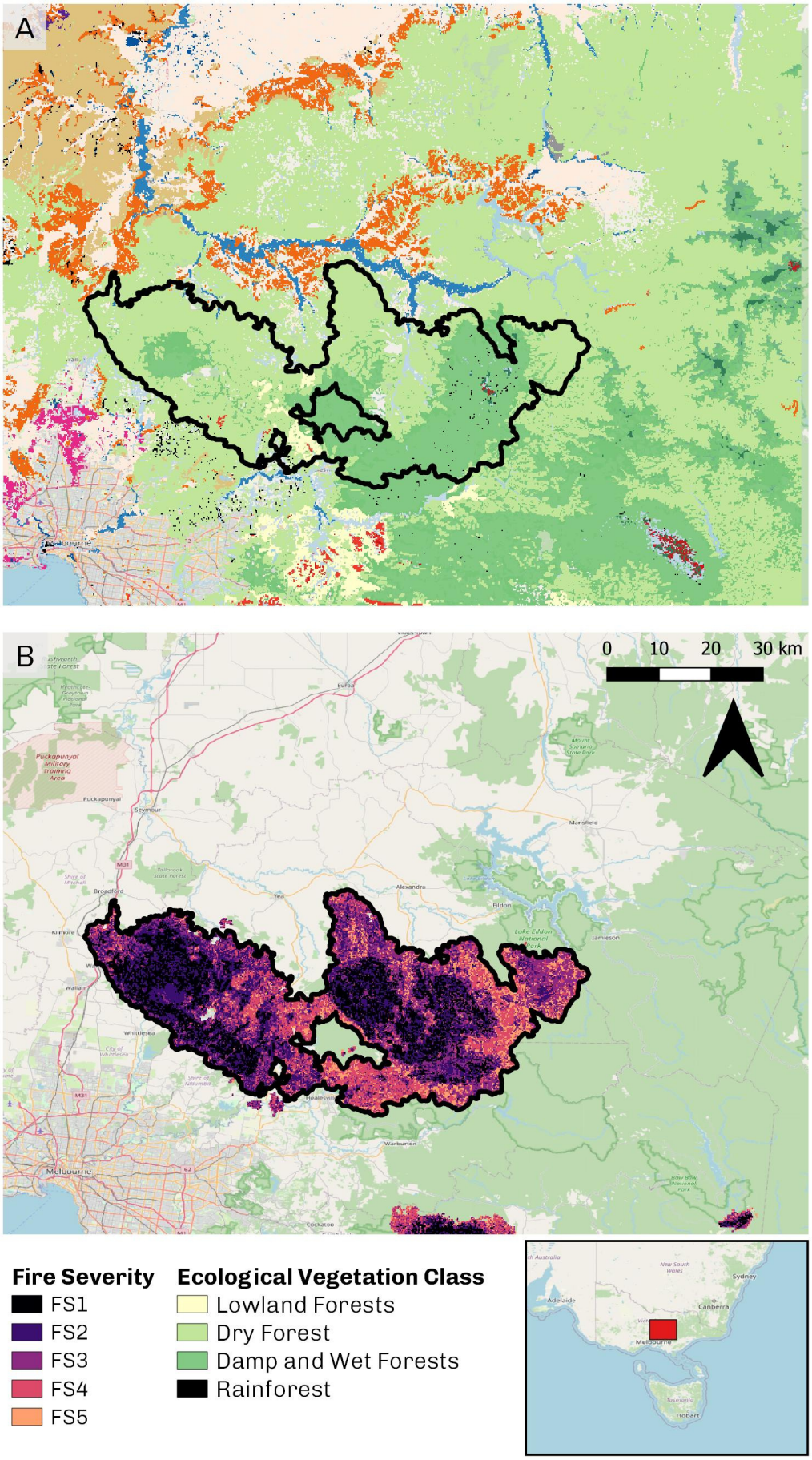

Figure 2.1: A: Ecological Vegetation Classes of the Killmore-Murrindi fire complex. Only the main vegetation classes in the burned area are presented in the legend. Within the study, the focus will be on the Dry Forest and the Damp and Wet Forest (referred to as Wet Forest). B: Fire Severity map of the Killmore-Murrindi fire complex. FS1 represents the most severe burn where the entire crown and understory are consumed. FS5 represents the least severe burn, where only the understory is affected. Both are the 250x250m rasterised versions of the data set as described in Section 2.2

.

Figure 2.2: From left to right: Dry Forest, Damp Forest and Wet Forest. These forest types spatially transition into each other from left to right with increasing rainfall and moisture availability. Eucalyptus trees grow quicker and taller with more water availability, resulting in taller and straighter trees in the Wet Forest (up to 75m compared to 30m in height in the Dry Forest). Within this study, Damp and Wet Forest are grouped together. Pictures are by Paul Gullan, 2017

Eucalyptus and forest fire

Eucalyptus is known for its resilience to forest fires, and can typically survive the most severe fires. The extent of the tolerance is typically thought to depend on the eucalyptus species. This typical discrepancy between species has also been found in ground research at the Black Saturday sites by Bennett et al. (2016) and Benyon and Lane (2013). The previously mentioned 'Ash types' have high mortality rates when their crowns are affected during the fire (>90% mortality). The mixed-species eucalyptus, also known as fire-tolerant eucalyptus, that are dominant in the Dry Forest and prevalent in the Wet Forest have higher survival rates, even when their complete crown has burned (Benyon & Lane, 2013). However, the survival of mixed species eucalyptus in fires that burn their crown (referred to as a high fire severity / FS1) depends on their size; the larger trees are significantly more likely to survive than medium and small-sized trees (Bennett et al., 2016). The intermediate fire severity where the crown is affected but not consumed proved to be the critical point for Ash-type survival, and the mortality was found to be different from plot to plot. In the lower fire severities (light or no crown scorch, only understorey consumption), tree survival was >75% in all eucalyptus types (Benyon & Lane, 2013). Bennett et al. (2016) also noted that mixed-species eucalyptus of all sizes had higher mortality during the Black Saturday fires than in other, similar wildfires. It is likely that the Millenium Drought negatively affected the health and resilience of the trees, especially in the Dry Forest (Bassett et al., 2015; Bennett et al., 2016). This also indicates that the tolerance of the generally fire-tolerant mixed-species eucalyptus is not boundless.

Despite different survival rates, eucalyptus trees typically have two regrowth strategies. Either a lot of seeds are released which germinate after the fire, creating a new cohort of young eucalyptus saplings. Or the tree resprouts from epicormic buds and lignotubers, which are present in the bark and the underground parts of the tree, respectively (see Figure 2.3). Trees can do these strategies simultaneously, but Ash type trees are thought to be obligate seeders, who depend solely on seed germination. However, Vivian et al. (2010) proposes that assigning certain recovery behaviour to certain species is incorrect as it depends on environmental factors which behaviour(s) the trees exhibit and that Ash-type eucalyptus can recover by resprouting if at least a part of the tree survived. This has also been shown by Benyon and Lane (2013), who found many *E. Nitens* which both survived and resprouted via epicormic buds, even though it is an Ash-type.

According to Bennett et al. (2016), the mixed species eucalyptus in the Dry Forest recovered from the Black Saturday fires through a combination of resprouting and regeneration from seed. At low fire severities, most trees exhibited an epicormic resprouting strategy. At the higher severities, epicormic resprouting was still the main survival mechanism of surviving trees of all sizes, with sprouts from both branches and stems. Nonetheless, there was also prolific seed regeneration at the higher fire severities, which five years after the fire led to a combination of old-growth trees with epicormic sprouts and many small stems resulting from the seeds germinated after the Black Saturday fires. Basal resprouting was uncommon in all fire severities. Karna et al. (2020) investigated the forest 7 years after the fire and found in high severity sites, despite epicormic resprouting and seedling regeneration, a decreased mean height (due to death of upper branch

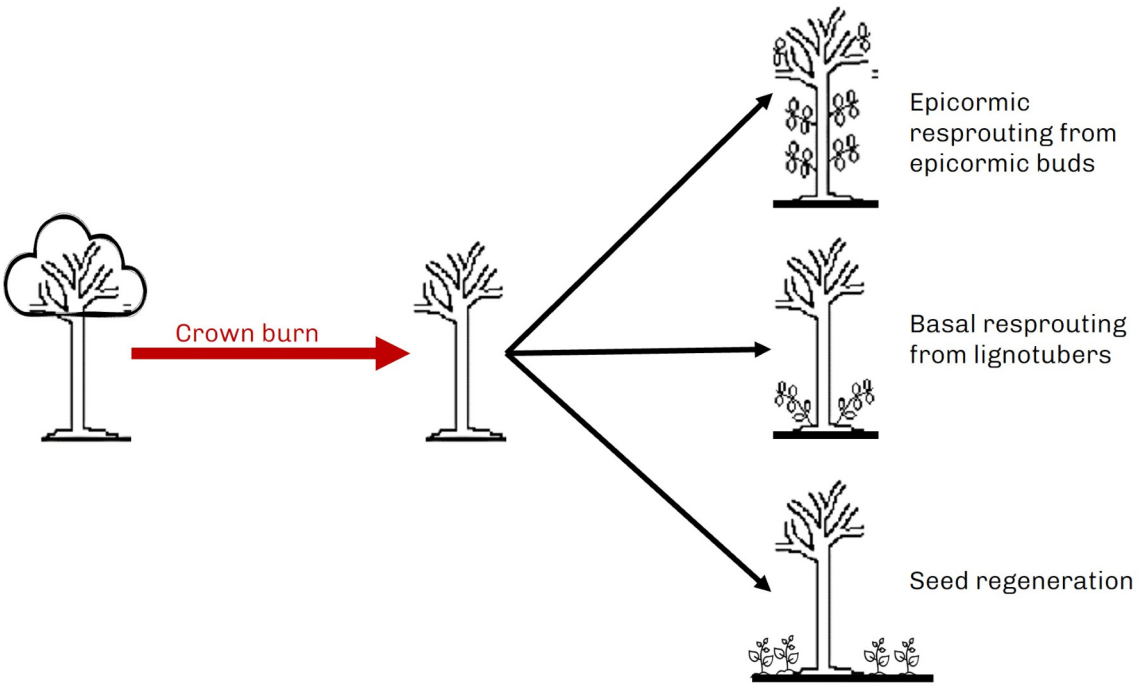

Figure 2.3: After a forest fire, eucalyptus trees can employ different regrowth strategies, which can occur separately or simultaneously. Mixed-species Eucalyptus (occurrence in both Dry and Wet Forest) typically recover via resprouting. Ash-type eucalyptus trees (prevalent in Wet Forest) tend to favour seed regeneration. However, the recovery behaviour depends on several factors including fire severity and environmental circumstances. Figure adapted from Vivian et al., 2010

epicormic buds), more heterogeneous and fragmented upper canopy and reduced cover. Those changes were not found in sites with low fire severities.

In the Wet Forest, where the overstorey is a combination of Ash-type eucalyptus and mixed species eucalyptus, Benyon and Lane (2013) found that the Ash-type trees had high mortality rates at high fire severities and recovered by seedling regeneration. However, the density of the seedling was very variable, and sometimes the ash eucalyptus seedlings were even absent. The ash seedling density differences were not related to fire severity, and thus ash seedlings also occurred at the low fire severity sites, where the mature ash eucalyptus had not died. The mixed species eucalyptus in the Wet Forest showed corresponding results to Bennett et al. (2016) findings. Additionally, for these tree species, a positive relation between fire severity and seedling density was found, and the seedlings that were in the lower fire severities were often sickly or dead in later surveys, due to competition and shadow. Understorey regeneration in the Wet Forest has been identified to be almost complete 2 years after the fire (Benyon & Lane, 2013).

In Figure 2.4, pictures are shown of these different recovery strategies. As this study investigates the fire effects in terms of scattering, it is interesting to note that these different recovery strategies will have different effects on canopy architecture and hence scattering from the vegetated surface. More importantly, they will look different in terms of scatterers than their undisturbed counterparts (Figure 2.2). It can also be seen that leaves have grown, whereas the structure of the forest remains heavily altered. Therefore, we hypothesise that the NDVI and ASCAT variables will have different responses in terms of recovery.

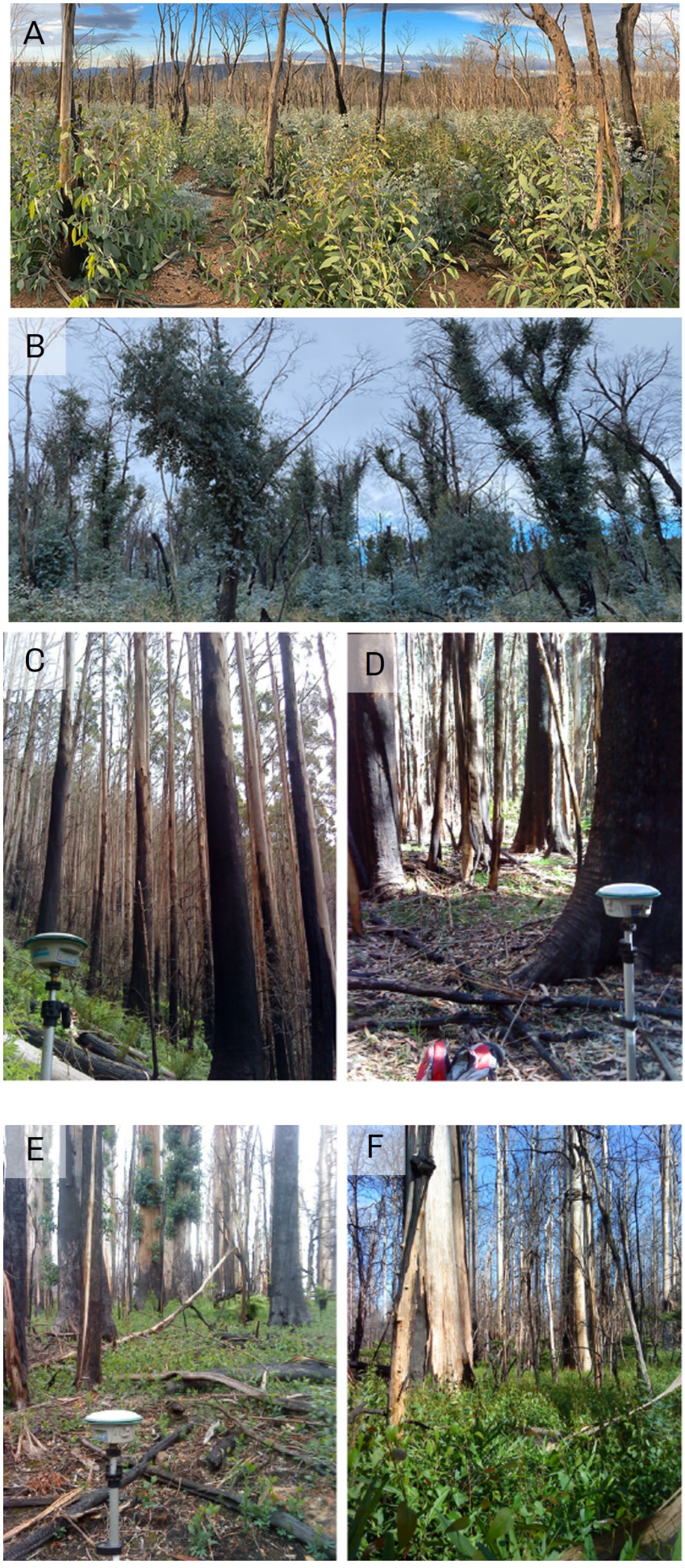

Figure 2.4: Different recovery behaviours exhibited by Eucalyptus trees.

A) The trees are not dead, but the epicormic buds were damaged too severely by fire, and therefore the trunk is unable to recover (i.e. dead). However, buds at the bottom of the trunk and buried lignotubers were protected and have been stimulated to grow as there is no longer top dominance that inhibits their growth. The trees have thus recovered per basal resprouting.

B) Trees were not killed and thicker bark protected the tissue holding epicormic buds to resprout. The only components that died were thinner branches at the top of the canopy

C & D) Living ash-type trees with only the understorey burnt.

E) Mature ash type tree which survived with epicormic regrowth and burnt understorey.

F) Fire-killed ash-type tree with prolific seedling regeneration.

Pictures A & B from Qin et al. (2022) taken 1 year and 2 months after the 2019/2020 Black Summer fires in a Dry Forest. Pictures C-F from Benyon and Lane (2013) taken 11-15 months after the Black Saturday fires in the Wet Forest

2.2. Data

In this section, the different sources of data are described. As the focus of the study is on the ASCAT data, the resampling of the other data sources to the spatial resolution of the ASCAT variables is described as well.

2.2.1. Advanced Scatterometer (ASCAT)

ASCAT is a scatterometer operating at a frequency of 5.4 GHz (C-band) on board of EUMETSAT's Meteorological Operational (MetOp)-A, -B and -C satellites, launched in 2006, 2012 and 2018, respectively. The ASCAT instrument has three antennas on each side (fore-, mid- and aft-beams) and these sets of antenna triplets allow for measurements at each grid point at multiple incidence angles.

Initially developed to account for vegetation influence and to normalise backscatter measurements σ^o to a common incidence angle θ in the TUW Soil Moisture Retrieval Algorithm, slope σ' and curvature σ'' have become a source of information of their own in recent years. The parameters were developed for normalisation of the ERS1/2 backscatter observations (Wagner et al., 1999). The instrument measured backscatter σ^o at three incidence angles (fore, mid and aft), which allowed for the calculation of the instantaneous incidence angle (θ) relationship for backscatter (σ^o). To evaluate these backscatter measurements at a common incidence angle, a second-order Taylor polynomial is used. Slope and curvature are the first and second derivatives of this polynomial (see Equation 2.1). This polynomial is rewritten and then used to normalise all backscatter measurements to a common reference angle ($\sigma^o(\theta_r)$) and to minimise vegetation effects.

$$\sigma^o(\theta) = \sigma^o(\theta_r) + \sigma'(\theta_r)\dot{(}\theta - \theta_r) + \frac{1}{2}\sigma''(\theta_r)\dot{(}\theta - \theta_r)^2 \quad [dB/deg] \tag{2.1}$$

To calculate the slope and curvature for this polynomial, a local slope is determined from the fore-, mid- and aft-beam measurements. When the ERS instrument was still used, these local slope measurements were used to determine slope σ' and curvature σ'' seasonalities, requiring several years of data for robust results (due to noise in local slope values) (Wagner et al., 1999). This also caused the inherent assumption that vegetation was inter-annually constant. However, vegetation has both inter- and intra-annual dynamics.

The newer ASCAT instrument created the opportunity to determine the slope σ' and curvature σ'' dynamically due to increased data density created by both the so-called 'backscatter triplets' (i.e. three more beams are added to the instrument compared to ERS1/2) and more sensors simultaneously being in orbit. Melzer (2013) proposed to dynamically calculate slope and curvature using an Epanechnikov kernel smoother on the local slopes (Figure 2.5). Hahn et al. (2017) demonstrated that the σ' and σ'' values were robust.

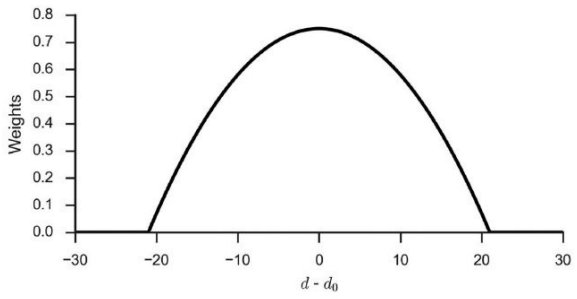

Figure 2.5: Slope and curvature are determined from a number of local slope measurements made by the backscatter triplets on the ASCAT instrument. To do so, an Epanechnikov window is used to smooth the measurements. In this example, a 21-day window is presented. In this study, a 31-day window is used to decrease high-frequency noise. Figure taken from Melzer (2013)

Vreugdenhil et al. (2017) described how the newly determined dynamic slope and curvature aid in monitoring dynamic vegetation using the vegetation optical depth. Later, Steele-Dunne et al. (2019) proposed the self-contained information potential of the now dynamically determined slope and curvature for vegetation phenology and vegetation water dynamics, instead of using it solely for the purpose of correcting for vegetation in the soil moisture retrieval algorithm or in determining vegetation optical depth. Pfeil et al. (2020) found the slope σ' to be sensitive to spring activation in deciduous forests.

Within the backscatter incidence angle relationship ($\sigma^o(\theta)$), slope and curvature change based on the dominant scattering mechanisms. If the soil is bare, surface scattering is dominant, creating a steep decrease of the backscatter signal at high incidence angles (i.e. only little of the signal scatters back). If there is more vegetation, volume and multiple scattering become dominant and the backscatter becomes increasingly incidence-angle independent. This effect flattens out at high incidence angles, or might even reverse, which is described by the curvature. An example of these differences is shown in Figure 2.6.

Microwave remote sensing such as the ASCAT backscatter is sensitive to two things in vegetation. Firstly, to wet above-ground biomass and the changes in it which describe vegetation dynamics. Secondly to the physical structure of the vegetation canopy and in the amount and distribution of scatterers in the vegetation (Pfeil et al., 2020). As the slope and curvature describe the relation between backscatter and incidence angle, they are partly sensitive to the same phenological changes. Slope describes the wet biomass of the vegetation and its scattering mechanisms. It is important to note that it is not directly related to vegetation greenness. A high slope (close to zero) describes a scattering mechanism that is largely incidence angle independent (volume and multiple scattering). Volume and multiple scattering are related to, but not necessarily the same as, high vegetation density. Curvature is less well understood but has been found to be influenced by vegetation structure and phenology. Steele-Dunne et al. (2019) established that curvature 'contains some information about vegetation independent of slope', where it is at least related to the vegetation geometry and the verticality of the vegetation structure. As mentioned before in Chapter 1, the interpretations of both variables are still somewhat unclear. For this study, they are assumed to mainly represent a change in scattering mechanism due to an increase or decrease of scatterers in terms of number, distribution, size and water content.

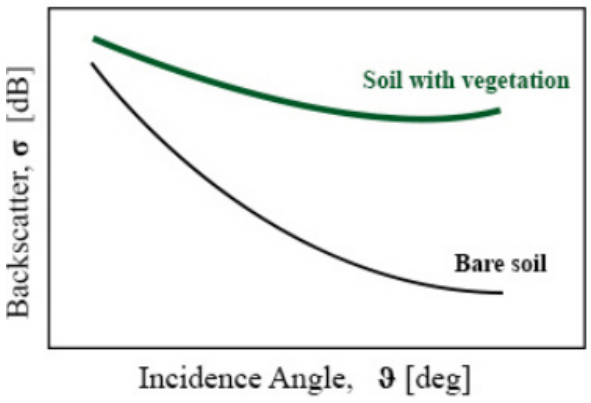

Figure 2.6: Example of how the backscatter incidence angle relation ($\sigma - \theta$) changes with increasing vegetation: the slope decreases as more of the signal scatters back at higher incidence angles. Slope values are negative and closeness to zero indicates increased volume and multiple scattering describing more vegetation. Curvature values surround zero and create either a convex (positive) or concave (negative) curve. This example shows a convex curve and thus positive curvature. Figure taken from Petchiappan et al. (2022)

In this study, ASCAT slope (σ') and curvature (σ'') time series are used from 01-01-2007 up to 31-12-2021 with a daily temporal resolution. The values have been created following Melzer (2013)'s methodology, using a kernel width of 31 days on the local slope values. This entails that each daily entry is calculated from the 62 days surrounding that day. A kernel of 31 days has been chosen to smooth out high-frequency behaviour which is not of interest in investigating impact and recovery. The data are resampled on a 12.5km swath grid to a fixed earth grid using a Hamming window function with a diameter of 23km (Naeimi et al., 2009; Petchiappan et al., 2022). The dataset is therefore considered to have a coarse spatial resolution, but a high temporal resolution. Due to the coarse resolution, the ASCAT data points are referred to as grid points. In total 143 grid points are considered in this study, later divided into affected and unaffected by the fire.

2.2.2. Moderate Resolution Imaging Spectroradiometer (MODIS)

Normalised Difference Vegetation Index (NDVI) was obtained from the Terra Moderate Resolution Imaging Spectrodiometer (MODIS) Vegetation Indices (MOD13Q1) Version 6.1 (Didan, 2021). The data are generated every 16 days at 250m spatial resolution as a level 3 product. Global vegetation indices have been computed from atmospherically corrected bi-directional surface reflectances that have been masked for water, clouds, heavy aerosols and cloud shadows. For the MODIS NDVI, the time series of 01-01-2007 up to 31-12-2021 have been selected as well. The images' low-quality pixels have been masked and assigned a value of -9999 using the DetailedQA band. Later, in resampling, the low-quality pixels have been assigned a NaN value. The scale of the product is 0.0001 and ranges from -2,000 to 10,0000.

In this study, NDVI data has been chosen to compare the ASCAT variables to, because it is one of the most conventional and useful parameters to investigate forest fire effects (Chuvieco et al., 2020; Pérez-Cabello et al., 2021). The knowledge of NDVI behaviour post-forest fire aids in the interpretation of the possible slope and curvature signals. Additionally, Veraverbeke et al. (2012) found that NDVI outperforms other VI's when investigating heterogeneous vegetation. As our study investigates the forest fire effects at a coarse spatial resolution, each grid point covers several vegetation classes, making it heterogeneous by default. Its suitability for eucalyptus forest has also been described by Heath et al. (2016), who mention that the vertical stance of the eucalyptus leaves and the foliage cover allow for light to penetrate through the canopy to the understorey and ground layers, due to which NDVI can be used to examine the changes throughout the entire communities vertical structure. Additionally, slope σ' and curvature σ'' have not been previously compared to NDVI, except for the notion that slope reacts to wet above-ground biomass rather than greenness, for which NDVI is considered a proxy. In this study, the NDVI acts as a benchmark and helps interpret the ASCAT variables.

2.2.3. Victorian Bushfires Severity Map 2009

The Victorian Bushfires Severity Map 2009 (Department of Environment, Land, Water and Planning, 2018b, Figure 2.1) has been taken from DataVic, Victoria's open data platform. It is a derived classification of a SPOT and Landsat TM woodlands fire severity index to map the fire severity of the February 2009 Victorian forest fires known as the 'Black Saturday fires'. The dataset has been validated by ground control as well as air photography. A fire severity map like this is used to quantify the degree of environmental change caused by fire, where it provides information on the loss of organic matter both above and below ground (M. A. Tanase et al., 2015). It is therefore a direct measure of impact.

Initially downloaded as a polygon dataset, it has been rasterised to a 250x250m grid by means of mode in the Google Earth Engine. This spatial resolution has been chosen to match the resolution of the MODIS NDVI.

The dataset contains six levels of fire severity: Fire Severity 1 up to 5 (FS1-5), where FS1 is the most burned and FS5 is the least burned. FS0 represents unaffected pixels. For simplicity, all FS0 pixels have been changed to FS6, such that the trend of 'higher FS, less burned' continues. FS4/5a is referred to as FS4, and FS5b is referred to as FS5. The scale is then as follows:

- Fire Severity 1 (FS1): Crown burn
- Fire Severity 2 (FS2): Crown scorch
- Fire Severity 3 (FS3): Moderate crown scorch
- Fire Severity 4 (FS4): Light or no crown scorch, understorey burnt
- Fire Severity 5 (FS5): No crown scorch, understorey slightly burned
- 'Fire Severity 6' (FS6): Unaffected by fire

2.2.4. Native Vegetation - Modelled 2005 Ecological Vegetation Classes

The 'Native Vegetation – Modelled 2005 Ecological Vegetation Classes' (Department of Environment, Land, Water and Planning, 2018a, Figure 2.1) maps the Native Vegetation extent with the Ecological Vegetation Classes (EVC), in which the classes are specifically collected for Victoria. The EVC dataset was multi-polygon data like the Fire Severity data. It has also been rasterised to a 250x250m raster using the Google Earth Engine, using mode. With several studies on the Black Saturday fires focusing on either Dry Forest or Wet Forest (Bennett et al., 2016; Benyon & Lane, 2013; Karna et al., 2020) and the other vegetation classes minimised in the rasterisation, the decision has been made to focus on the Dry and Wet forest solely.

2.2.5. Data Pre-Processing

As the focus of this project is on the ASCAT grid points and their post-fire behaviour, all other data are resampled to those points. For the resampling, a 23km Hamming window is used, as the ASCAT data has also been processed with such a window. The resampling function used is based on the resampling function in the Pytesmo package (Paulik et al., 2022). The function has been altered to handle NaN inputs differently than the original function did. In the original function, if there was only 1 NaN value in any of the neighbours, the entire resampling was given a NaN value. In the new function, the neighbours with NaN values were assigned zero weight and thus ignored. This was especially important for the NDVI data which contained many NaN values due to quality control.

The Hamming window used 8646 250x250m pixel neighbours for each ASCAT grid point. It is used to resample the NDVI, the rasterised Fire Severity and the rasterised Vegetation Classes. The NDVI has been resampled to the ASCAT grid point for each temporal entry. For the Fire Severity and Vegetation Classes, the Hamming window was used to calculate the fraction of each class, where more weight is assigned to pixels close to the ASCAT grid point location than those far away by means. These fractions are later used to determine the Burn Scale, the affected grid points of interest and potential control grid points.

The grid points of interest have been selected by the rules below. The resulting affected grid points and their corresponding fire severity distribution are shown in Figure 2.7. To be able to compare the affected grid points to an unaffected counterpart, potential control grid points are determined as well. The potential control grid point selected here are later used to determine the control grid points per affected grid point following a Time Series Similarity (TSS) approach. For the best TSS results, the potential control grid points are not selected according to their vegetation class (also see Section 2.3.2 and Appendix B).

- **Dry Forest Affected Grid point**: 'FS1 + FS2 + FS3 + FS4 + FS5' > 50% & Dry Forest > 65%
- **Wet Forest Affected Grid point**: 'FS1 + FS2 + FS3 + FS4 + FS5' > 50% & Wet and Damp Forest > 65%
- **Potential control gridpoints**: 'FS1 + FS2 + FS3 + FS4 + FS5' < 50% & FS1 < 2%

With all the data now resampled, the following is available for each ASCAT grid point:

- Time series from 2007 up to 2021 with daily entries for slope σ' and curvature σ''
- Time series from 2007 up to 2021 with 16-day entries of resampled NDVI data
- Fire Severity fractions
- Ecological Vegetation Class fractions

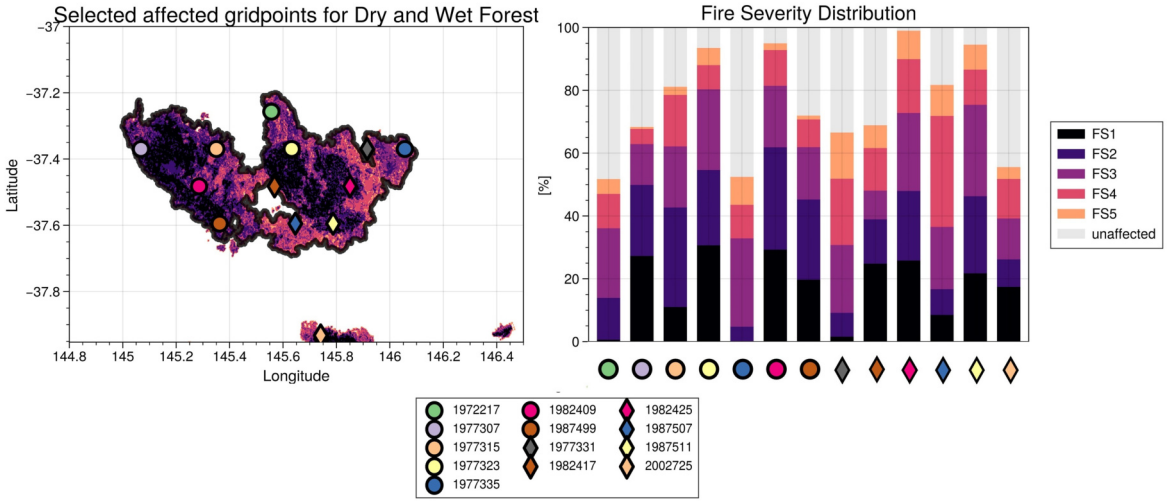

Figure 2.7: Selected affected grid points of interest for both Dry Forest (7 grid points, circles) and Wet Forest (6 grid points, diamonds) and their corresponding fire severity distributions. All grid points of interest are at least 50% burned and contain 65% of their respective vegetation class. Legends correspond to both figures.

2.3. Methodology

In this section, the methods of the study are discussed. This includes the newly introduced variable Burn Scale to describe the fire severity in the coarse spatial resolution that is used. Secondly, the data analysis that is done to investigate the response of the ASCAT variable and the NDVI to the fire is discussed.

2.3.1. Burn Scale

With the resampling of the fire severities to the ASCAT grid points, fire severity distributions are available for each grid point (as seen in Figure 2.7). To be able to compare the fire severity of each grid point to each other, the Burn Scale has been developed. This scale has been designed to include both the total percentage % of the 23km radius area burned, as well as the severity with which it burned. In Appendix C other options for possible Burn Scales are explored. From the different options, the Burn Scale presented here appeared to be the most adequate.

The developed and chosen burn scale is calculated following Equation 2.2. The translation of fire severity distribution as seen in Figure 2.7 into Burn Scale is as shown in Figure 2.8.

$$\text{Burn Scale} = \frac{(\%\text{ high severity} \times 4) + (\%\text{ moderate severity} \times 3) + (\%\text{ low severity} \times 2) + \%\text{ Unaffected}}{100} \tag{2.2}$$

where:

- % high severity = fraction fire severity 1 + fire severity 2
- % moderate severity = fraction fire severity 3
- % low severity = fraction fire severity 4 and 5

Dry Forest Grid points	Burn Scale	Wet Forest Grid Points	Burn Scale
1972217	2.0	1977331	2.1
1977307	2.8	1982417	2.6
1977315	2.9	1982425	3.2
1977323	3.3	1987507	2.3
1977335	1.9	1987511	3.2
1982409	3.4	2002725	2.2
1987499	2.8		

Figure 2.8: For each affected grid point, the fire severity distribution of Figure 2.7 has been translated into the Burn Scale using Equation 2.2. The Burn Scale includes both the % affected as well as the fire severity. A Burn Scale > 3 is considered to be high and a Burn Scale < 2.5 is considered to be low.

The decision to divide in high, moderate and low has been made based on other research using a similar categorical system (Bennett et al., 2016; Benyon & Lane, 2013; Karna et al., 2020; Lentile et al., 2007; M. Tanase et al., 2015). Nonetheless, there are many other categorical systems used (for example, see Bassett et al., 2015; Heath et al., 2016; Leonard et al., 2014). It is also interesting to note that Fire Severity 3 (i.e. moderate severity) is the critical severity for eucalyptus tree survival (Benyon & Lane, 2013). For this research, a similar categorical division was not adequate, as the area that one ASCAT grid point describes is never homogeneously burned (nor completely burned) due to its coarse spatial resolution. Therefore, a continuous scale that encompasses both the percentage % affected as well as the severity was most suitable.

The interpretation of this scale is reversed from the fire severity. It is such that if the Burn Scale is at its maximum of 4, the entire area described by the grid point would be completely burned in the highest fire severities. If the Burn Scale is 1, the area is completely unaffected.

With the Burn Scale, it is possible to see if the degree to which a grid point has been damaged has an effect on the impact and recovery. As the fire severity describes the damage done to the forest, it is already a measure of impact and thus logically remotely sensed time series would show different impacts for different fire severities and consequently different Burn Scales values. This notion is enhanced by the fact that (spectral) remote sensing change detection techniques are used to create fire severity maps, including the fire severity map used here. Microwave remote sensing has been found to be able to distinguish between fire severity classes as well (M. Tanase et al., 2015), thus we hypothesise that the ASCAT variables show distinct impact responses to different fire severities as well. Fire severity also has a well-established relationship with post-fire recovery (Turner et al., 1998), where higher fire severities remove the capacity of the burnt areas to recover, whereas less severely affected areas are often followed by rapid recovery (João et al., 2018). Fire severity especially influences the long-term recovery, whereas short-term recovery is more heavily influenced by the vegetation type and abiotic factors such as precipitation and the temperature (João et al., 2018).

Although the conscious choice has been made to create the Burn Scale due to the coarse spatial resolution of the ASCAT grid points, it does eliminate the separate fire severities. Therefore, it makes the physical interpretation of the impact and recovery of the forest and the different variables more difficult, which was already complicated due to the coarse resolution of the data themselves. Nonetheless, in the interpretation, we assume that a high Burn Scale (>3) represents the same thing as the high fire severities (FS1 & FS2). For a low Burn Scale (<2.5), we assume behaviour similar to the low fire severities (FS4 & 5). For these, we do not assume the area to be unaffected as all grid points of interest are already selected on being >50% affected. Both the terms such as high fire severity and high Burn Scale will be used in the interpretation and comparisons of the results.

2.3.2. Work Flow

To investigate the impact and recovery due to the fire, it is important to compare the affected grid points to unaffected grid points. Out of several possible methods, Time Series Similarity (TSS) was chosen. One reason is that quickly recovering vegetation types such as eucalyptus forest (Qin et al., 2022) might undergo recovery that is not captured by a bi-temporal comparison method, where the results largely depend on image acquisition time and seasonal timing. Another reason is that TSS eliminates external influences such as plant phenology and seasonality (which have been identified in the individual time series, see Appendix A) (Lhermitte et al., 2010). With this method, a measure of "what would have been, had the fire not happened" is established.

The TSS method used in this research is based on Lhermitte et al. (2010), however, the method has been simplified as several steps were deemed unnecessary working with coarse spatial resolution grid points instead of high-resolution pixels. For each affected grid point (the focal grid point), its time series is compared to the time series of all unaffected grid points in the two years before the fire. The unaffected grid points that have the most similar time series are selected as the control grid points. Then after the fire, the focal grid point can be compared to these selected control grid points, in which it can be assumed that if they were similar before the fire, they would have remained similar after the fire and that thus any deviation is caused by the fire.

Throughout the explanation of the workflow that follows, visual examples are provided of a slope time series of an example focal grid point. Those examples are shown in Figure 2.9 and 2.10.

Control grid point selection

For each variable time series:

1. Select the 2 years before the fire (2007-02-07 — 2009-02-06) in all grid points (affected and unaffected).
2. Calculate the Root Mean Square Deviation (RMSD) between the time series of each affected grid point and all unaffected grid points.
3. For each affected grid point, select the corresponding nine unaffected grid points with the smallest RMSD. The choice for nine grid points has been made after runs of trial-and-error, as well as to prevent dividing by (almost) zero later in the process.

For this process, note that the selection of the nine control grid points is done separately both for each focal grid point and for each variable (i.e. slope, curvature and NDVI). There is also no RMSD cut-off, as inspection of the results showed that the RMSD values were well below the cut-off set by Lhermitte et al. (2010). The last thing of importance is that the control grid point selection is not based on the vegetation class of the unaffected grid points, because it both defies the concept of Time Series Similarity, as well as that it increased pre-fire RMSDs, and thus selected control grid points that were a worse fit. Inspection of the selected control grid points showed that control grid points were often not of the same vegetation class as the focal grid point. This deviation can also be seen in Figure 2.9. A further investigation is presented in Appendix B.

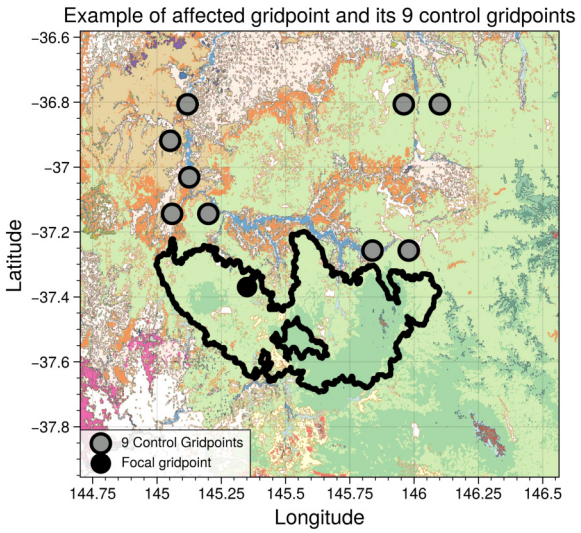

Figure 2.9: Spatial overview of the example affected grid point (black) and its nine selected control grid points for the slope variable (grey). The control grid points have been selected using RMSD-based time series similarity on the slope variable the 2 years before the fire.

Z-score

As a means of comparison between the affected grid points and their selected control grid points, a Z-score is calculated. The Z-score is a standardised measure of how many standard deviations the affected time series is away from the average of the nine selected control grid points. This measure of comparison is chosen because it is expressed in standard deviations rather than in variable units, which makes the variables slope, curvature and NDVI comparable (despite their different units and magnitudes).

The Z-scores of the time series are calculated both for the entire time series (i.e. daily Z-scores for the curvature and slope, and 16-day interval Z-scores for the NDVI), as well as annual Z-scores, where the Z-score is the average of each year since the fire (i.e. 2009-02-07 — 2010-02-07). This is done to further reduce seasonal influences and to increase the signal-to-noise ratio. With the annually averaged Z-scores, the most basic signal as a result of the fire is obtained. The calculation of the Z-score is according to Equation 2.3.

$$Z = \frac{x_{af,t} - \mu_{unaf,t}}{\sigma_{unaf,t}} \tag{2.3}$$

where t either is an entry of the entire time series, or represents the average of an entire year since the fire.

If $Z = 0$, the affected grid point is similar to the control grid point average. If this occurs after the fire, the affected grid point can be regarded as recovered. However, the pre-fire Z-score is non-zero for all focal points in all three variables, and thus we interpret a Z-score close to zero as recovered as well. The translation of the original time series into a Z-score time series is presented in Figure 2.10a and Figure 2.10b, where it is also visible that the pre-fire Z-score is non-zero. The non-zeroness is typically a result of small standard deviations rather than actual deviations in the variable. See for example the 2007 peak in Figure 2.10b which reaches about 5 standard deviations, compared to the drop of about minus 3 standard deviations following the fire (red line). If you inspect these in Figure 2.10a, the difference between the variables is larger following the fire than in 2007, but the standard deviation in 2007 is very small causing a large Z-score. It is important to keep this in mind when interpreting the Z-score values. The annually averaged Z-score values are shown as black circles in Figure 2.10c. The effect of the different standard deviations appears to be reduced when averaging over the year.

Comparison and interpretation of Z-score time series

Although the TSS method should produce very small Z-scores pre-fire (as the chosen control grid points are the most similar ones to the affected grid point in question), the Z-scores are non-zero pre-fire as shown before. This is paradoxically both due to the control grid point not being exact matches, as well as to small standard deviations because the chosen control grid points are the best matches possible. This creates difficulty in comparing the Z-score time series of different affected grid points.

To simplify comparing the different Z-score time series, a common reference is created. All annually averaged time series are corrected for their 'one year prior to the fire' value (2008). After this correction, whenever the Z-score reaches zero, it means that it reaches the level of similarity it had in the year before the fire. This means that now time series that had a different pre-fire Z-score can be compared to each other. The annually averaged corrected time series of the example grid point can be seen in Figure 2.10d.

The interpretation of the Z-score time series is done in terms of impact and recovery. With impact, we refer to a deviation from zero after the fire. With recovery, we refer to an evolution of Z-scores to zero. Note that both these concepts are qualitative rather than quantitative. Nonetheless, they are adequate for the means of our study. From the different impacts and recoveries, we try to establish general findings on how slope and curvature respond to fire, and how that behaviour relates to the NDVI response. To make the comparison between the variables intuitive, all variables are displayed on an equal y-axis even though the variables have different magnitudes. The impacts and recovery are also compared to each other in terms of the Burn Scale as discussed before.

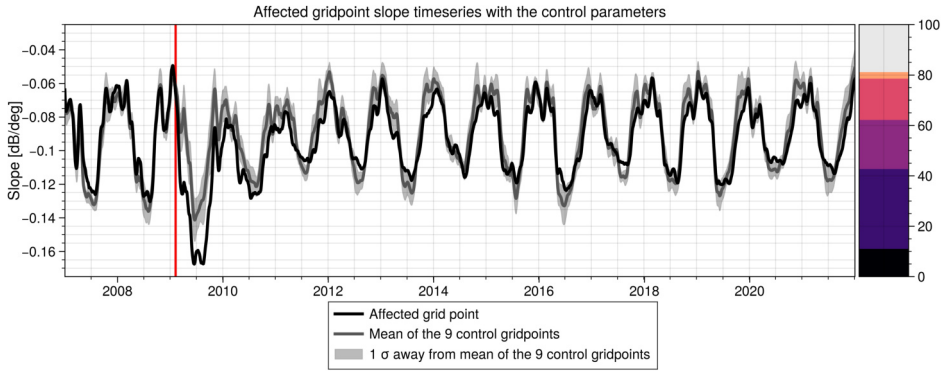

(a) The slope time series of the example affected grid point (black line), shown with the average slope time series of the nine selected control grid point time series (grey line) and the standard deviation of these control grid points (grey shading). The control grid points have been selected using an RMSD-based time series similarity approach based on the 2 years before the fire.

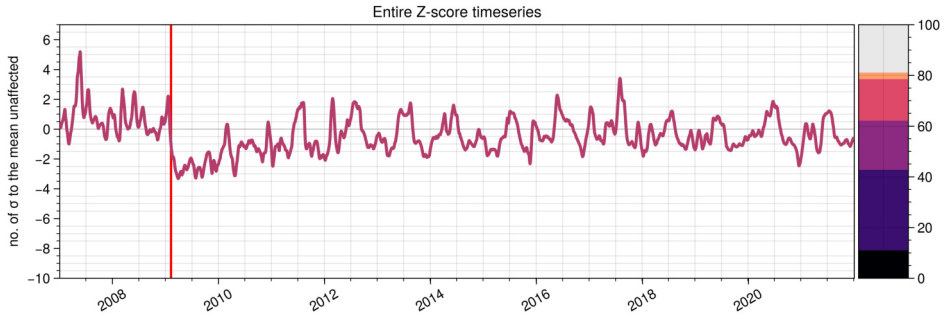

(b) The Z-score time series of the example affected grid point, calculated using Equation 2.3 and the slope time series, mean and standard deviation as seen in Sub-figure 2.10a. The pre-fire Z-score is non-zero due to exaggerations partly caused by small standard deviations.

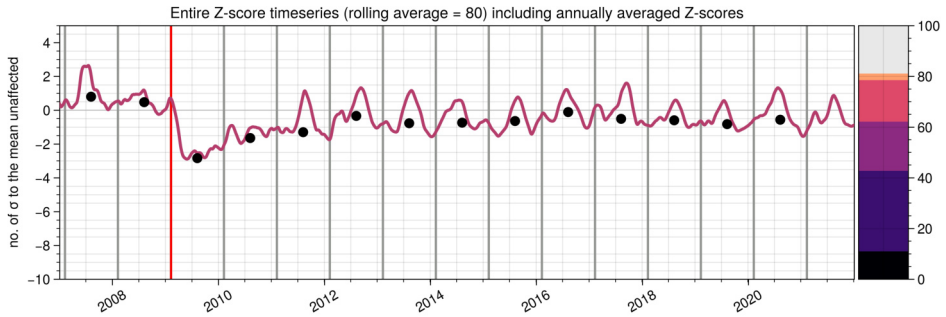

(c) The Z-score time series for the slope of the affected example grid points. Presented with a rolling average of 80 days. The black dots represent the annual averages starting each year at the 7th of February. Both the rolling average and annual average are tested in minimizing noise in the Z-score time-series.

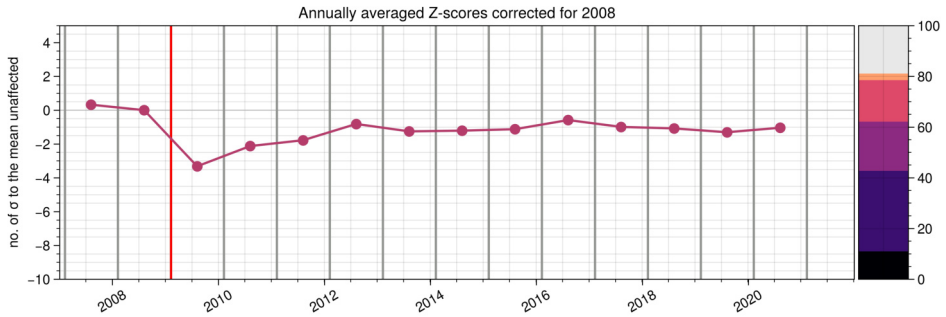

(d) The annually averaged Z-score for the slope time series of the example affected grid point. This annually averaged time series has been corrected for the year 2008, which is now at zero, to simplify comparing different time series to each other.

Figure 2.10: The figures represent from top to bottom the translation of a raw variable time series into an entire daily Z-score time series (b) and an annually averaged and corrected Z-score time series (d). In all sub-figures, the date of the fire has been presented in red. The fire severity distribution of the example affected grid point is presented in the right bar.

2.3.3. Impact Analysis

To quantify the relation between Burn Scale and impact, a linear regression between the two has been performed. However, to do so, the impact had to be more strictly defined than previously. For this analysis, the impact has been defined using the entire time series as seen in Equation 2.4.

$$\text{Impact} = \mu(Z_{\text{31 days—93 days, post-fire}}) - \mu(Z_{\text{93 days— 31 days, pre-fire}}) \tag{2.4}$$

The temporal distance from the fire is used to account for the kernel effects within the slope and curvature. The decision to average two months is to decrease noise. An example of the selection is shown in Figure 2.11. Linear regression is then performed with the Burn Scale and this newly defined impact to see whether there is a relation between the two. A relation is assumed to be significant if $p < 0.05$.

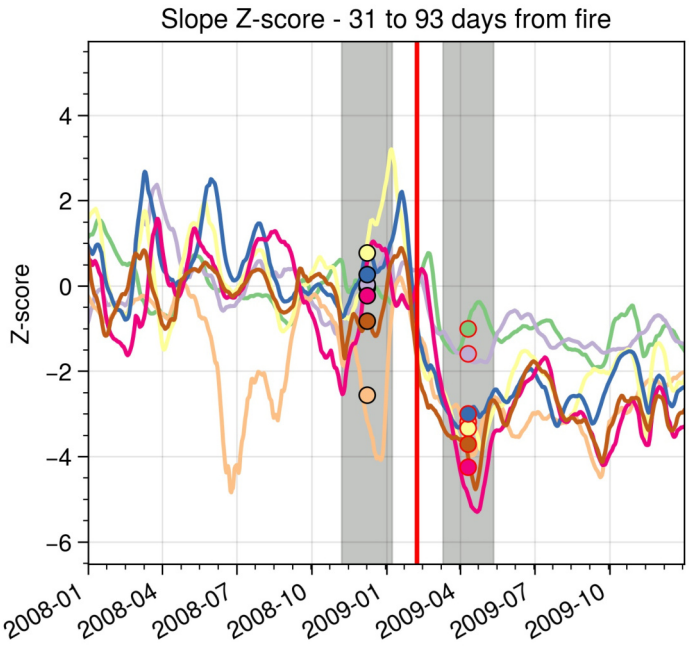

Figure 2.11: The pre- and post-fire averages on slope Z-score time series for the impact analysis, which uses an alternative impact definition. The date of the fire is shown in red. The grey boxes represent the period from which the pre- and post-fire averages are calculated. The pre-fire averages describe the period from 3 months before the fire up to 1 month before the fire. The post-fire averages describe the period from 1 month after the fire up to 3 months after the fire. The temporal distance to the actual fire date is to omit kernel effects in the ASCAT variables.

3

Results

3.1. Entire Time series

The entire Z-score time series are presented in Figure 3.1, which will be discussed in terms of impact and recovery below.

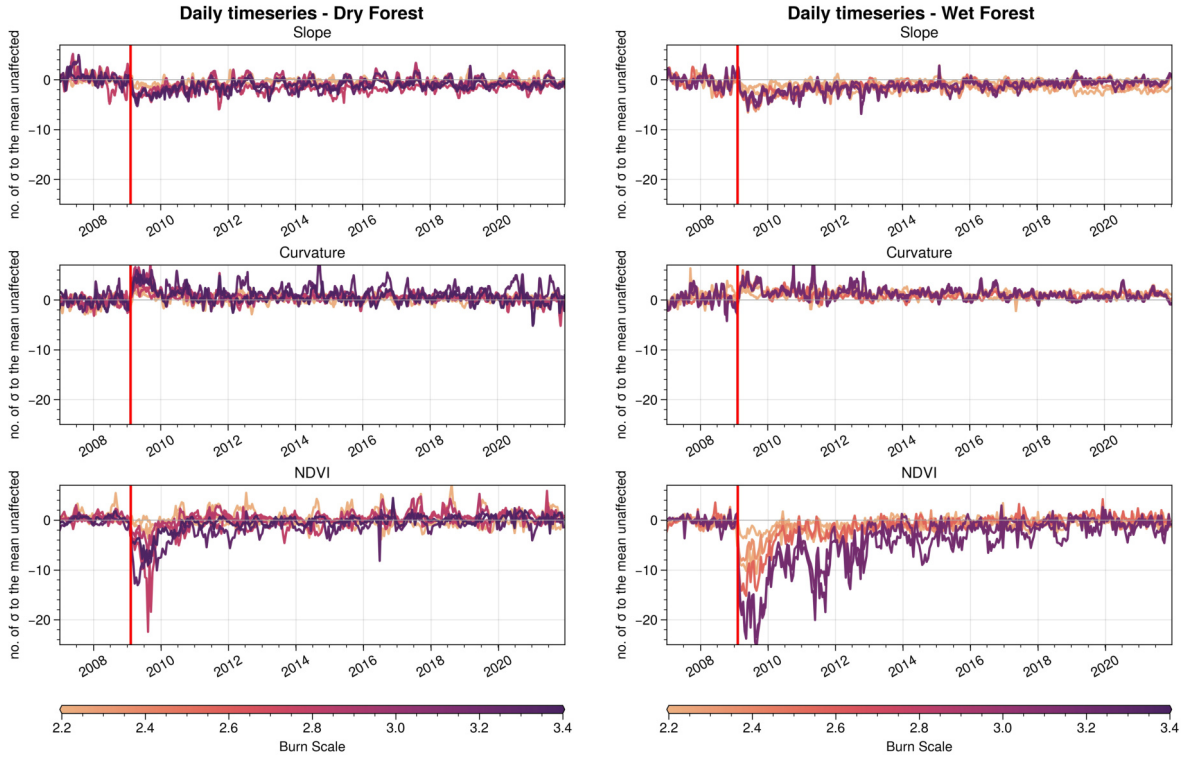

Figure 3.1: The entire Z-score time series. Each grid point is separately coloured based on its Burn Scale value. For the slope and curvature, the Z-scores are daily. For the NDVI, there is an instance every 16 days. The red line presents the date of the fire. All three variables show an impact shortly after the fire and later a recovery by evolution towards zero. The recovery appears to be divided into two phases, with a phase of quicker recovery visible in all variables (2 years for the Dry Forest, 4-5 years for the Wet Forest). After this period, the NDVI is centred around zero and recovered to the signal's original state, whereas the ASCAT variables have a slow recovery up to the end of the study period.

3.1.1. Impact

In all three variables and all grid points, a drop (or increase in the case of curvature) occurs shortly after the fire (red line), where the Z-score deviates from zero, especially when compared to the pre-fire Z-score. The magnitude and exact timing differs between variables as well as between grid points. For the NDVI, it is known that this drop is related to vegetation loss during the

fire, as that same effect has been shown before (See for example Heath et al. (2016), Lhermitte et al. (2011), and Qin et al. (2022)). The ASCAT variables show similar behaviour as the NDVI, it can therefore be assumed that the change in the Z-scores is a measure of vegetation change due to the Black Saturday fires. This assumption is reinforced by the ASCAT variables being understood as a representative of vegetation (in terms of structure, above-ground biomass water content and in some sense vegetation density), as well as the fact that microwaves are able to detect fire impact in eucalyptus forest (Fernandez-Carrillo et al., 2019).

For the slope, a negative Z-score means that the burned forest has decreased volume and multiple scattering compared to its unburnt counterparts. Both in high severity fires as well as in low severity fires, scatterers are lost. For example, everything from the understorey, leaves and small branches up to small and medium trunks can be consumed in fire, depending on variables such as fire severity and tree age. The loss of these scatterers causes a decrease in volume and multiple scattering, and thus a decrease in the slope in the affected grid points compared to the unaffected control grid points. There is no distinct difference in slope Z-scores between the Dry and the Wet Forest, besides the Wet Forest being slightly more negative.

For the curvature, a positive Z-score means that the curvature became more positive in the burnt forest than in its unburnt counterparts. Curvature values are typically around zero: slightly negative in a forest and slightly positive in grassland (Hahn et al., 2017). The curvature in the study area is continually positive for most grid points (see Appendix A), which is unusual for a forest. Forest is typically thought to have negative curvature, but it is very structure dependent, hence the positive curvature in the Eucalyptus forest. A possible explanation for the positive curvature here is that mature Eucalyptus trees hold their leaves vertical instead of horizontal (Heath et al., 2016), causing vertical scattering at high incidence angles and thus positive curvature values. The distinct vertical structure of the Eucalyptus trees possibly also contributes to the positive curvature values; the trees are often very tall and straight with branches only occurring higher up in the tree.

However, that would not explain why the curvature becomes increasingly positive after a fire. A possibility is that the increase in curvature is due to another vertical scatterer becoming more dominant. For example in the higher fire severities, leaves and branches combust (Keith et al., 2014), but the large vertical tree trunks remain. Another possible explanation would be that the forest generally starts resembling a grassland more after the fire (which typically has positive values), however, most eucalyptus forests are very resilient in fires and do not burn down completely, as discussed in Chapter 2, which makes this option less likely.

The NDVI shows a negative Z-score after the fire, which is in line with for example Heath et al. (2016) and Qin et al. (2022) who describe decreasing NDVI values following eucalyptus fires. This impact is larger and the magnitude differs more between the two forest types than it does in the ASCAT variables. Two things could explain the magnitude of the impact:

- Leaves are more easily affected during a fire than structural components measured by ASCAT variables: in a fire, the leaves will be consumed before the branches. In all fire severities, leaves are affected, either only in the understorey or in the overstorey as well. The vertical leaves of the Eucalyptus trees allow the NDVI to measure understorey greenness and vigour to a certain extent (Heath et al., 2016). This means that in all grid points a (large) portion of the leaves is affected, which the NDVI can pick up. This consequently causes a NDVI Z-score impact. The slope and curvature react to volumetric scatterers which are not as easily impacted by the fire, especially in the lower Burn Scales. These variables thus exhibit a smaller impact than the NDVI, as less of what they measure is gone.
- A possible second reason for the large impact the NDVI shows are small standard deviation values for the unaffected grid points. The standard deviations of the NDVI control grid points are relatively smaller than for the slope and curvature, and the NDVI values of the forest are typically more spatially homogeneous. The closer-to-zero pre-fire Z-scores also suggest this homogeneity. If a variable generally is so homogeneous, a small impact already becomes a large deviation in terms of Z-score.

So the NDVI measures something more heavily impacted as well as that these impacts are enlarged by its original homogeneity.

In a zoomed version of the time series (Figure 3.2), it becomes apparent that there is no clear peak of maximum impact after which the Z-scores immediately start to recover, as well as that there is a delay of impact. This is the case for all three variables in both forest types. The delay can be partly explained by the fire burning for three consecutive weeks (although most damage is done in the first 12h) (Cruz et al., 2012). For the slope and curvature, the kernel width of 31 days influences the delay of the impact as well. These reasons can however not explain the entirety of the delay.

A possible explanation is that the heat and the following drought preceding the fire also impacted the unaffected control grid points. Drought impacts the variables in similar ways as fire does (Qin et al., 2022; Walraven, 2021). It might thus be that the preceding heat influenced the variables of the unaffected grid point as well. The unaffected grid point would then recover swiftly once the extreme weather conditions started receding. However, their affected counterparts stay behind in this recovery due to parts of the vegetation and resources being gone. This discrepancy would increase the difference between affected and unaffected grid points and thus enlarges the Z-score only at a later point in time. Analysis of the actual time series and ranges of unaffected grid points in Appendix A endorses this theory, as there is a change in unaffected grid points after the fire as well in the same direction as the affected grid points. Another possible explanation is that it takes some time for the impact to take full effect. For example, when most of the canopy is combusted in high severity fires, scorched leaves may remain in patches (Keith et al., 2014). Later, these leaves are dropped, possibly before epicormic resprouting and regrowth of leaves take off. Dead branches and stems are also known to collapse after the fire has passed (Bassett et al., 2015). Thus, it could explain why the delay is seen in all three variables. However, a clear conclusion cannot be made on the delay, but with the high temporal resolution of the ASCAT variables it might be interesting to investigate the delay further.

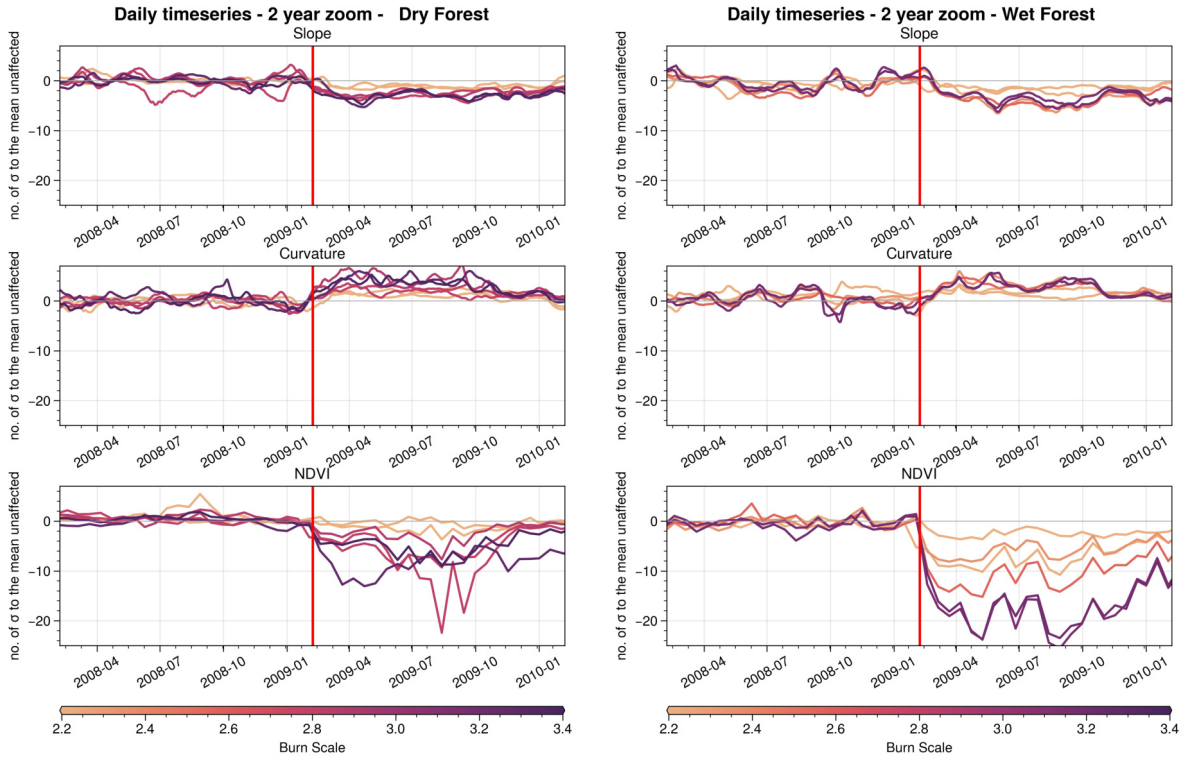

Figure 3.2: Zoom of the time series on a year pre- and post-fire to investigate the timing and magnitude of the impact. It is apparent that there is no clear peak of impact. There also is a delay in the impact of all variables. The red line indicates the date of the Black Saturday fires

3.1.2. Recovery

In all variables, there is an evolution from the impact towards zero in the years following the fire. If the Z-score is zero, the affected grid points are similar to their unaffected counterparts. In all variables and in most grid points, there is an initial steep recovery in the first few years after the fire, meaning that it is moving towards $Z = 0$ (i.e. full recovery) quickly, already starting in the first year. This period of steeper recovery is aligned in timing for all variables but differs between the two vegetation classes. In the Dry Forest, the period is clearest and spans about 2 years. In the Wet Forest, the alignment is less clear but takes about 4 or 5 years. Such a period of steep recovery starting almost immediately after the fire corresponds to findings by Qin et al. (2022) who found a large recovery in both passive microwaves as well as optical variables a year after the 2019/2022 eucalyptus forest fires. A steep recovery like this can be attributed to the resilience and quick growth of the Eucalyptus species. The growth of epicormic shoots (i.e. volumetric scatterers) already start months after the fire (McCaw et al., 1994), so it is no surprise that there is not only a steep recovery in the NDVI but in the ASCAT variables as well. Additionally, Benyon and Lane (2013) found that the understorey achieved complete regeneration after two years, which corresponds to the period of steeper recovery in the Dry Forest. A possible explanation is that the steep recovery is a combination of both under- and overstorey recovery, whereas afterwards the understorey no longer contributes to the changes and thus the recovery pace slows.

At the end of this initial period of steeper recovery, the NDVI is almost completely recovered to its original level (most grid points are at or close to $Z = 0$), whereas the ASCAT variables continue to recover up to the end of the study period, albeit slowly compared to the initial period of steep recovery. With this separation, two phases of recovery can be distinguished in the ASCAT variables, where the first represents quick recovery, followed by a longer period of slower recovery. These phases can also be recognized in the individual time series in Appendix A.

At the end of the study period, for most of the grid points the ASCAT variables have not reached the original state. This becomes more apparent when comparing the Z-scores to the pre-fire Z-scores. For example, Dry Forest Slope is close to $Z = 0$ but remains negative, whereas the Z-score used to be positive before the fire. It is debatable whether $Z = 0$ or the pre-fire Z-score is the best indicator for recovery. In this study, we assume $Z = 0$ to be the indicator for recovery, but it is wise to keep the pre-fire Z-score in mind.

The difference in time to reach recovery between the NDVI and the ASCAT variable can be explained by the fact that NDVI responds to vegetation greenness and vigour, whereas the ASCAT variables measure structural components of the forests. During recovery, leaves are quickest to regrow, both on the first epicormic sprouts on the eucalyptus trees, as well as from quickly resprouting understorey species. These young leaves and shoots can create an NDVI signal similar to the NDVI signal the mature canopy of the control grid points exhibits, hence appearing recovered. This does not mean that the recovered NDVI is a complete restoration of the pre-fire canopy. The slower structural components indicate this. With quickly growing understory and the epicormic sprouts, structural components start to grow quickly as well, but the amount and distribution of scatterers of this young regrowth is nothing alike the original structure (see for example Figure 2.2 and Figure 2.4). As shown in the time series, it takes many more years before the ASCAT variables show a recovered state, where the canopy is structurally similar to its unaffected counterparts. However, the ASCAT variables describe a combination of the number of scatterers, their distribution, water content and size. At the end of the study period, the combination of these things is (almost) similar to its unaffected counterparts. It is still possible that the forest looks different if you would physically visit it. Yet, the recovered ASCAT is more likely to represent a state of the forest that looks similar in the field than a recovered NDVI, or at least functions in a similar way as the original forest.

The swifter recovery of the NDVI compared to the ASCAT variables is in line with findings by Karna et al. (2020) who compared LiDAR measurements with NDVI measurements seven years after the Black Saturday fires, and noted that the forest had recovered in greenness (NDVI), but not yet structurally. That the ASCAT variables are close to recovery at the end of the study period

can be once again attributed to their resilience and quick regrowth. With epicormic resprouting, a eucalyptus forest can be recovered structurally in 10-15 years (Qin et al., 2022) which is the time span of our study. The earlier recovery of NDVI compared to structural variables is not in line with Massetti et al. (2019), where they found that the NDVI, NBR and the empirically-derived structural spectral index VSPI (which measures the amount and structure of the vegetation's woody biomass) were all recovered 2 years post Black Saturday Fires. Interestingly, this 2 year period seems to correspond to the period of steeper recovery that was identified in the Dry Forest. For many other fire complexes, Massetti et al. (2019) found earlier recovery for NDVI than for the VSPI.

The Burn Scale does not influence the short-term recovery, which is in line with João et al. (2018) their findings. The steep period of recovery is visible in all grid points regardless of their Burn Scale. At the end of this period, the Z-score levels of all Burn Scales are close to each other and thus the magnitude of recovery differs in this period, but not the timing. After this short-term recovery period, there is little influence of the Burn Scale with regard to recovery. Less severely burned grid points do not typically appear to be recovered earlier or further, especially for the ASCAT variables. For the NDVI, this is unexpected as João et al. (2018) mention that long-term recovery is especially related to fire severity. For the ASCAT variables, it is less unforeseen that there is little difference between high and low Burn Scale Z-scores, as Fernandez-Carrillo et al. (2019) made a similar observation, and explained that it is not necessarily a lack of difference in recovery, but a matter of proportionality. On the matter, they write: "*the recovery of few vegetation elements may contribute proportionally more when starting from low backscatter values (e.g. only stems in areas with high fire severity). Conversely, in areas affected by low-moderate severities, enough scattering elements are still present in the tree canopy, making proportional backscatter gains smaller for the same quantity of recovered elements. It might also be the case that, in areas affected with low-moderate severity, trees have a lesser need to generate new scattering elements at a fast pace*" *(p.140)*.

3.2. Annually averaged time series

As can be seen in Figure 3.1, the original Z-score time series contain a lot of noise. To increase the signal-to-noise ratio, the time series have been reduced to annual averages as described in Chapter 2. The results are presented in Figure 3.3.

3.2.1. Impact

All variables and all grid points show an impact in the year of the fire (except for one grid points its ASCAT variables in the Wet Forest). For slope, the magnitude of impact is equal between the two forest types. For curvature, the Dry Forest now shows a more heavy impact than the Wet Forest. In the NDVI it is the other way around, the Wet Forest is more heavily impacted than the Dry Forest. In this representation, there is a clear positive relation between the Burn Scale and the Z-score impact. This is further explored in Section 3.4.

3.2.2. Recovery

The earlier discussed period of an initial steeper recovery is still visible in the annually averaged time series. This period of steep recovery might be a result of eucalyptus communities requiring post-fire rainfall to ensure growth and development. This is especially true for seed regeneration, but resprouting favours wet conditions for growth as well (Heath et al., 2016). The year 2010 (one year post-fire) was the first year that broke the Millenium Drought. The year 2011 was an especially wet year in Victoria, Australia, with a lot of rainfall in late SH Summer. This wet summer is captured in both +1 and +2 years after the fire, which are also the points one could decipher as steeply recovering years, especially in the Dry Forest. These favourable growth conditions post-fire and the quicker-than-normal recovery both in spectral and structural indices were mentioned by Massetti et al. (2019) as well. Additionally, João et al. (2018) found short-term recovery to be related to climatic conditions such as precipitation and temperature, rather than to fire severity.

In the Wet Forest, most grid points are recovered +10 years post-fire, nonetheless, the Z-score drops again a year later (increases for curvature). This last year can most likely be attributed to other phenological effects that have nothing to do with the fire anymore. It is therefore debatable whether the Wet Forest is recovered at the end of the study period or not. Nevertheless, it shows that the TSS-Z-score combination is not perfect in eliminating other effects in the comparison between affected and unaffected grid points. This could also have been identified from the non-zero pre-fire Z-scores.

In the Dry Forest, this effect between the 10th and the 11th year after the fire is not visible. Most grid points have a recovered NDVI at the end of the study period, of them, the time series generally reach $Z = 0$ for the first time in the 7th year after the fire. This corresponds to findings by Heath et al. (2016): they studied the NDVI recovery of fire-tolerant resprouting eucalyptus communities and found that the NDVI had recovered within 5 to 7 years. Acknowledging that their study its definition of recovery might be different, the timing corresponds to the NDVI recovery we see in the Dry Forest. In the Wet Forest, the NDVI recovery is slower. It is unclear what causes this slower recovery, especially as Karna et al. (2020) found the Dry Forest to undergo a slower recovery than the Wet Forest (for structural parameters). The slower recovery might also be an artefact of the small standard deviations in the homogeneous Wet Forests (and its control grid points), creating a large Z-score and exaggerating the impact remaining in the Wet Forest.

In general, it can be concluded that the NDVI signal is recovered by the end of the study period and that the ASCAT variables are nearing recovery, albeit slowly in the latter years of the study period. These generalisations are more astute for the Dry Forest than for the Wet Forest. These findings correspond to typical recovery signals for NDVI and structural parameters in eucalyptus forests (Heath et al., 2016; Karna et al., 2020) (and to a lesser extent to Massetti et al. (2019)'s general conclusions, which did not hold for the Black Saturday fires). It is debatable to what extent full recovery is necessary to continue performing the pre-fire ecosystem services. However, Benyon and Lane (2013) mention that the water quality and yield in these forest catchments remain affected for up to 30 years after a fire, which implies that there is even more time needed for a full recovery. M. Tanase et al. (2011) mention that it can take decades for a forest to reach the biomass level, structure and carbon sink capacity of the forest pre-disturbance.

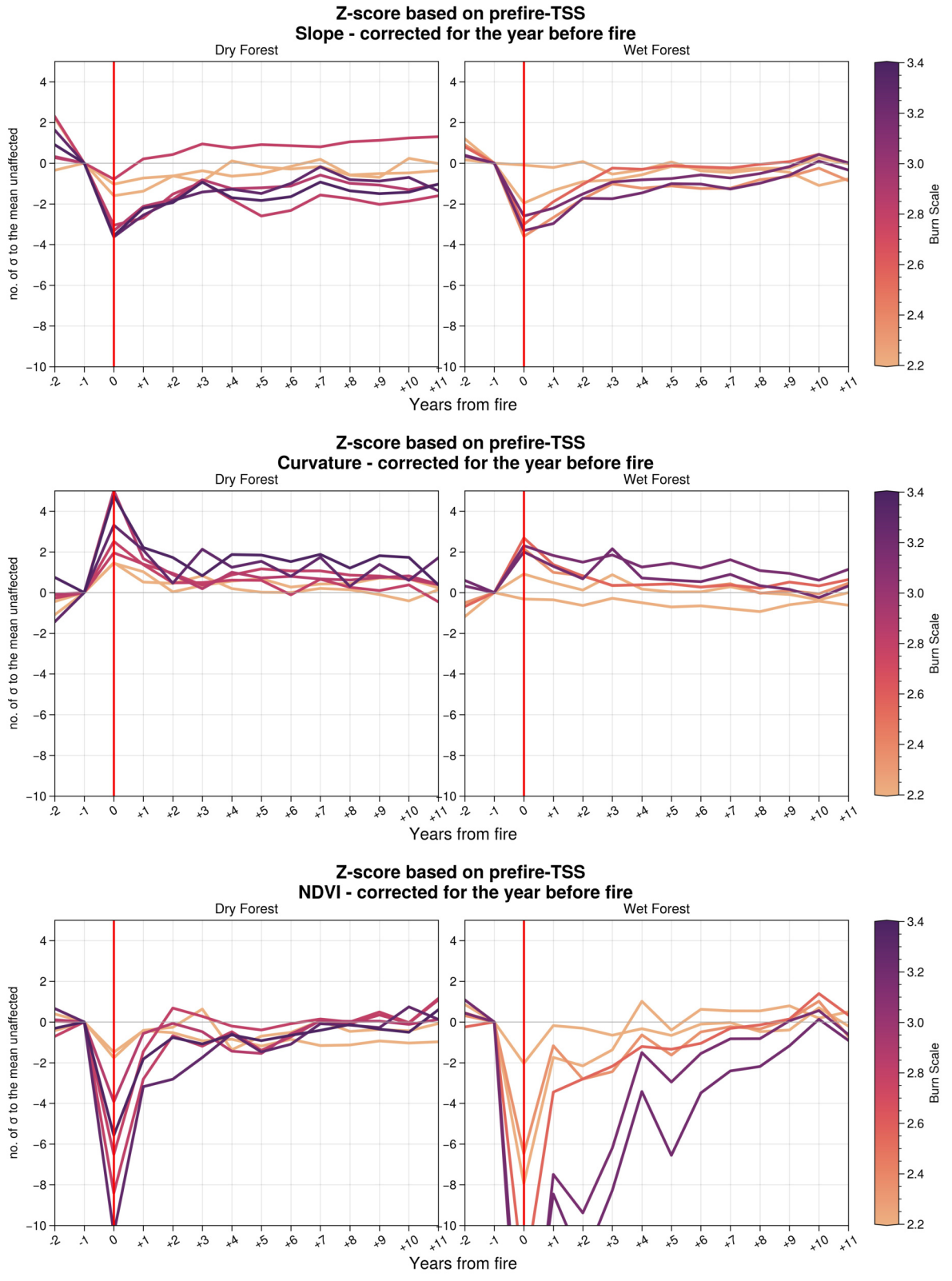

Figure 3.3: Annually averaged time series where each year since fire describes a year between the consequent 7th of Februaries. Time series are corrected for the value at one year prior to the fire. The impact shows a positive relationship with the Burn Scale. The difference in recovery between the ASCAT variables and NDVI is more apparent than in the daily time series. Two different phases within the recovery can still be recognised in this visualisation.

3.3. Pair plots

The pair plots as shown in Figure 3.4 provide a different perspective more focused on the correlation between the three different variables. It also shows recovery in terms of time without the entanglement of the Burn Scale of individual grid points.

3.3.1. Impact

Within the scatter plots, most of the grid points are closely grouped together. However, the year of the fire (black points) is separated from this group. This shows the impact as shown before. The histograms show that the year of the fire has the largest range, which becomes increasingly smaller over time. This initial range can be attributed to different fire severities.

3.3.2. Recovery

In all variables, a noticeable recovery can be seen where the points become closer over time to the [0,0] point (where both the variables are recovered). Later years are mostly grouped, it is then no longer clear that the later, the closer to recovery the forest is. From the scatter plots, it cannot be said whether the grid points have reached recovery at the end of the study period.

The relation between the ASCAT variables and the NDVI is curved, describing a quicker recovery for the NDVI, while the ASCAT variable lags behind. This is more apparent in the Dry Forest than in the Wet Forest. The slope and curvature are more linearly related in their recovery. The swifter recovery of the NDVI can also be seen in the histograms, where for the NDVI the peaks of the latter years are very high and narrow and thus the Z-scores are very homogeneous. At the end of the study period, narrow NDVI peaks are centred around zero, describing that all grid points are at or close to recovery. These high and narrow peaks already show after 3 years (Dry Forest) and 5 years (Wet Forest). These could thus be seen as the respective recovery periods, which are shorter than the time series analysis indicated but are close to what was identified as the steep recovery period.

For the ASCAT variables, the peaks become narrower over time, but remain broad compared to the NDVI, indicating a larger discrepancy in recovery between the individual grid points. The peaks of the later years are not centred around zero like the NDVI. However, the centre of the latter years in the Dry Forest curvature is closer to zero than its slope counterparts, indicating that on average the curvature is further recovered than the slope. In the Wet Forest, the centres of these later years are offset from zero about the same for slope and curvature, but the slope peak is higher and narrower, so more decisively close to zero than the curvature is.

The pair plots analysis confirms the swifter recovery of NDVI compared to the ASCAT variables. This analysis also showed that at the end of the study period the NDVI of all grid points is at a similar stage of recovery, while for the ASCAT variables, there is more discrepancy in how far along they are in their recovery.

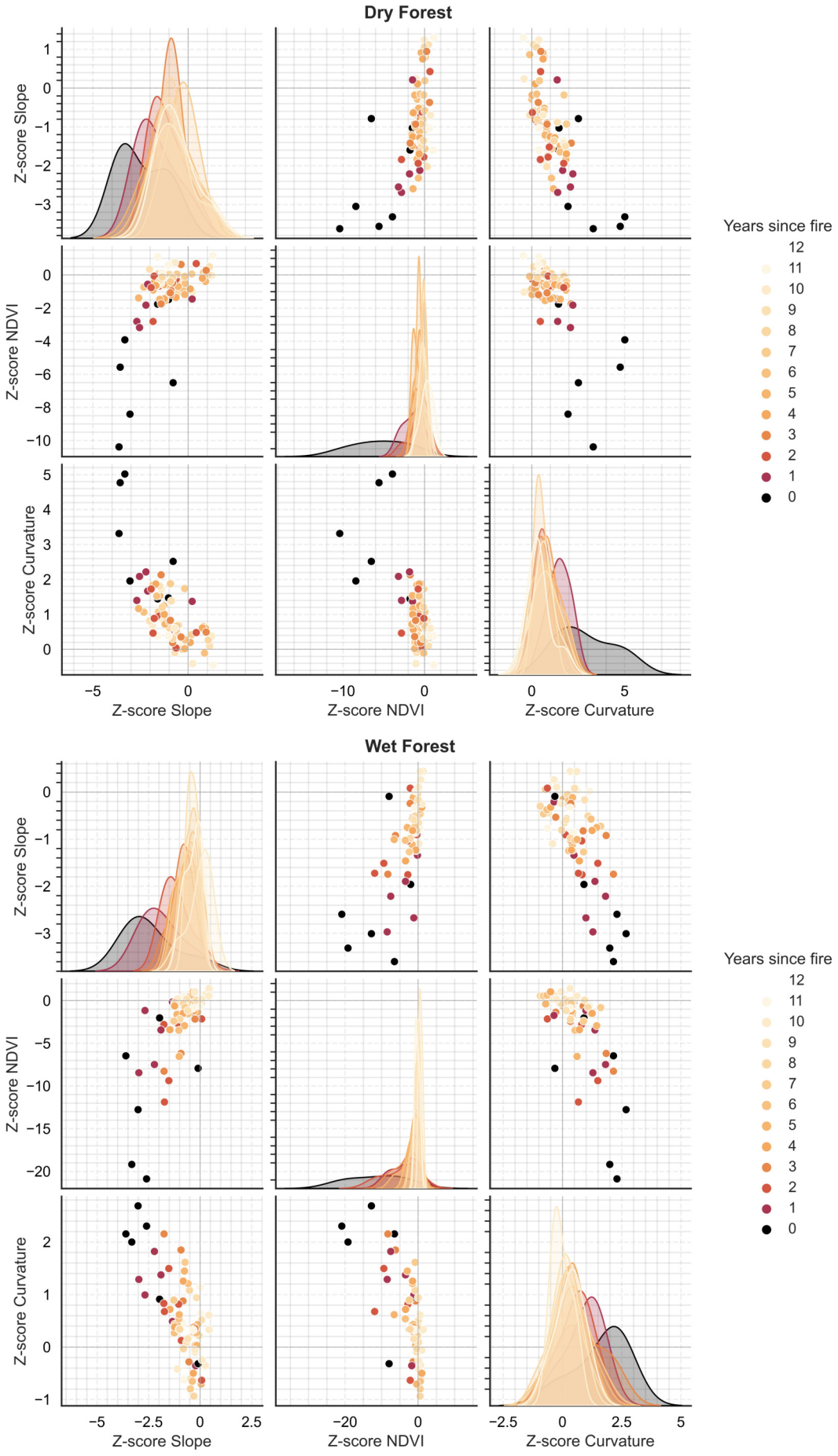

Figure 3.4: Pairplots for the Dry (top) and Wet Forest (bottom), coloured by years since the fire. The histograms show the Z-score distribution of each year. In this alternate visualisation, the location [0,0] describes both variables to be recovered. The ASCAT variables and NDVI show a curve, describing a difference in recovery timing. The narrow peak of the NDVI histograms compared to those of the ASCAT variables show a quicker and more complete recovery as well.

3.4. Impact Analysis

As suggested before, there appears to be a positive relationship between the Burn Scale and the Z-score impact. Earlier it was found that there is no clear point of impact. Additionally, the nature of the eucalyptus forest and its quick recovery starting only months after the fire, make that the annual average at year zero does not represent the damage done by the fire adequately. For this section, the impact is defined as the difference between the average of 1-3 months after the fire and the average of 1-3 months before the fire. Further explanations can be found in Chapter 2. The results are shown in Figure 3.5.

In all variables, there is a positive relationship between Burn Scale and impact, describing a larger impact with increasing Burn Scale. For the NDVI, this relation is clearer than for the ASCAT variables. It is significant for the Wet Forest NDVI. The relationships are not very strong, and not significant for the most part. Nevertheless, the occurrence of matching relationships in all variables indicates that the impact is affected by the Burn Scale.

The clearer relationship for the NDVI can be explained by the fact that the Burn Scale is based on a fire severity map that is based on optical imagery. The fire severity map is therefore mostly an indicator of the severity in terms of colour rather than structure. Although not significant for the most part, there still is a relation between the Burn Scale and the impact of the ASCAT variables (and thus that the ASCAT variables show differences between fire severities). This is because fire severity, even when based on optical imagery, represents damage. Damage to a forest during a fire includes the loss of scatterers, which will be measured by the ASCAT variables. This relation is in line with efforts by M. Tanase et al. (2015) to develop fire severity mapping based on L-Band SAR, who found good results but call for better ground observations based on scatterers instead of colour for better calibration.

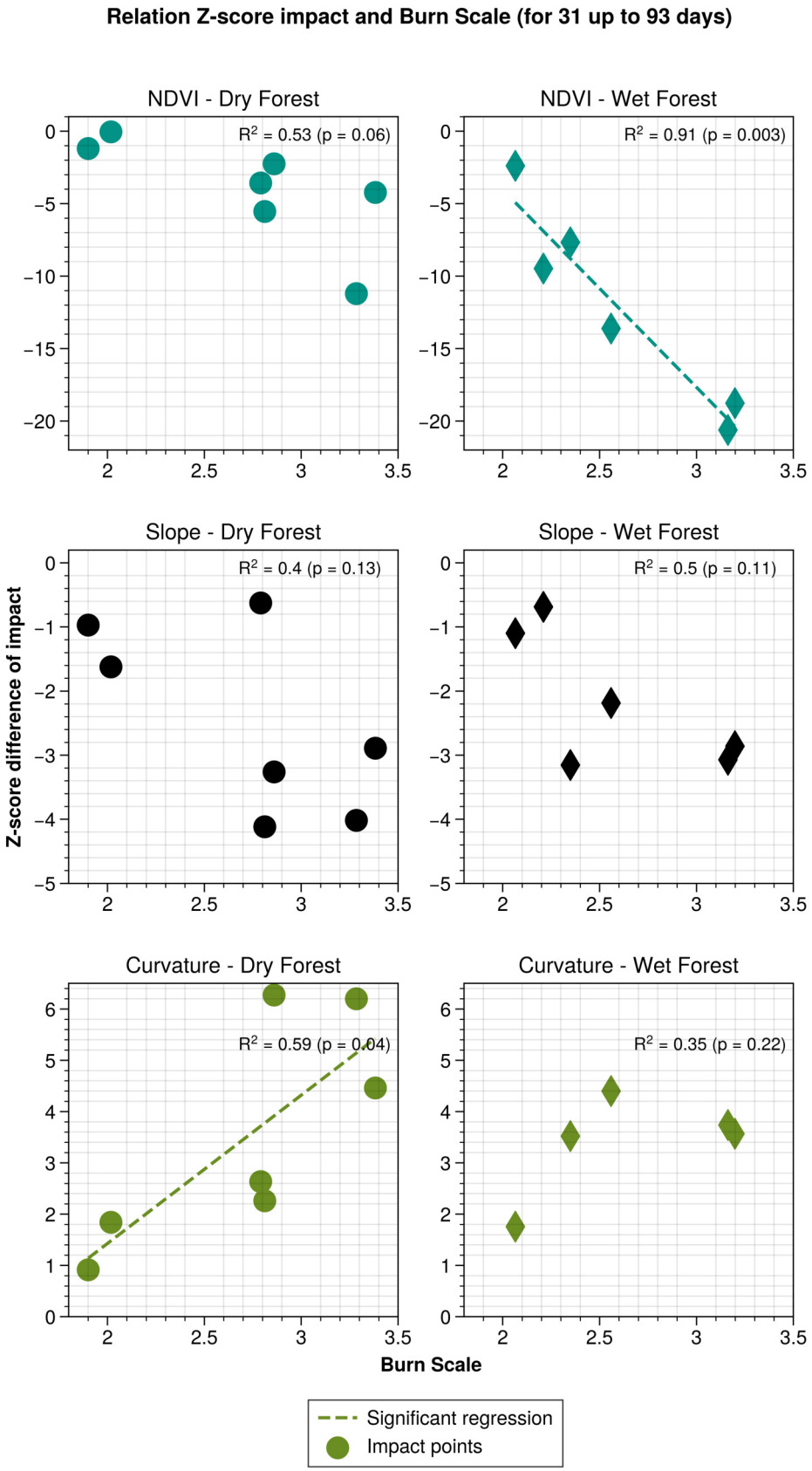

Figure 3.5: Burn Scale vs. Z-score difference of impact. The impact has been determined with Equation 2.4. For each variable and each forest type, R^2 values and Pearson coefficients are presented. Pearson's coefficients <0.05 are considered significant. Significant relations are presented as dashed lines. The variables show a positive relationship between the Burn Scale and the impact. It is however not significant for most of them.

4

Discussion

In this study, the goal was to establish how the ASCAT variables slope σ' and curvature σ'' respond to forest fires, and whether they showed an impact and a recovery. To do so, grid points that were affected by the Black Saturday fires were compared to similar unaffected grid points. Herewith, the sensitivity of the ASCAT variables to forest fire impact and post-forest fire recovery has been confirmed. The impact was shown by the time series deviating from zero shortly after the fire due to a loss of scatterers in the fire. Over time, the time series evolved back towards zero depicting a recovery as scatterers grow back in the vegetation. These results confirm the suitability of the ASCAT variables as self-contained sources of information on vegetation, as suggested by Steele-Dunne et al. (2019). To interpret the ASCAT results and confirm that their signal was related to the forest fire, the results were compared to a similar analysis of the commonly used forest fire indicator NDVI. The NDVI analysis presented the same general results. This confirms that the signals seen in the ASCAT variables are a response to the forest fire. An important difference between the NDVI and the ASCAT variables was the timing of the recovery of the signal. The results were in line with other studies evaluating eucalyptus forest fires with remote sensing techniques. In-field assessments after the Black Saturday fires could be related to the time series as well.

The finding that both ASCAT variables are sensitive to forest fire effects contributes to the research on the understanding and applicability of these variables. Both variables are not that well understood yet and discovering to what kind of vegetation processes they are sensitive aids in understanding them. One understanding of slope and curvature is that their variations represent changes in the number, distribution, size and moisture content of scatterers and consequently the scattering mechanisms. For this study, that understanding was assumed and used to interpret the results. This decision was made because forest fires are known to remove scatterers and regrowth is characterised by the return of scatterers (Fernandez-Carrillo et al., 2019; M. A. Tanase et al., 2013). As the slope and curvature are shown to go through an impact and recovery, the assumption that changes in these variables represent changes in the scatterer numbers, size, distribution and moisture content is enforced.

These results are especially interesting for the curvature, as it is assumed to be a combination of fitting noise of the second-order polynomial and actual self-contained information. Steele-Dunne et al. (2019) found the curvature to be a self-contained parameter in grasslands with information on vertical scattering and structure. This study presented that the curvature shows a clear impact and recovery related to the forest fire. This enforces the idea that curvature is more than fitting noise and also shows that it provides useful information in forests, additionally to grasslands. The increase in curvature that the forest fire causes is hypothesised to relate to an increase in vertical scattering as well, where possibly the remaining vertical trunks become more dominant in the backscatter response. The results are promising for curvature as a variable.

Considering the study from an ASCAT product development perspective, the results provide novel insight that the variables are sensitive to forest fire impact and recovery. In analysing the results, knowledge of forest fires was useful in the interpretation and in better understanding the behaviour of the variables. However, looking at the study from the forest fire research perspective, the results are currently less insightful. This is because we currently need forest fire knowledge to understand the ASCAT signal. Once the ASCAT variables are better understood, the contrary could be achieved: using the variables to remotely learn about a forest fire and its recovery, suppressing the need for time and cost-consuming in-field assessments. Before this becomes true, it is important to understand the limitations of the current study. These will be discussed in the following few sections.

4.1. Spatial Scale

The ASCAT variables and resampled NDVI exhibit the post-fire signals despite its scale of a 12.5km grid. This shows the sensitivity of the ASCAT variables and NDVI to vegetation changes but complicates spatial analysis as well as physical interpretation.

In forest fire research, it has become increasingly important to not only delineate the burned area but also to investigate the spatial heterogeneity of the damage (Chuvieco et al., 2020; João et al., 2018; Leonard et al., 2014). It is also known that the recovery is not homogeneous and depends on several factors both related to the fire severity and the landscape (João et al., 2018). However, with the coarse spatial resolution of the ASCAT variables, a lot of information on this heterogeneity is lost both in the impact and the recovery. For the impact, an attempt to preserve it has been done by down-sampling the fire severities and translating them into the Burn Scale. While it is true that the ASCAT variables' impacts were related to the different Burn Scale values, there will not be much use in using the ASCAT variables in investigating spatial heterogeneity, as the heterogeneity of interest is usually of a smaller scale. Additionally, in this study, a major forest fire has been investigated. Most forest fires burn a smaller continuous area, where the current spatial scale would be of less use. In a quick spatial comparison of the ASCAT variables and the resampled NDVI to the original higher resolution NDVI, it became immediately clear that many of the smaller scale spatial differences in both impact and recovery are not captured in the coarse resolution data, but that the general trends are equal. Capturing these heterogeneities is important as less severely burned or unburned patches are important for the recovery of a forest (Leonard et al., 2014).

For this study, the ASCAT variables are used to investigate impact as well as recovery, which are both limited by the coarse spatial resolution. However, in impact monitoring and active forest fire detection, remote sensing data with high temporal resolutions are preferably used (Chuvieco et al., 2020). The ASCAT variables are daily variables and although they are currently computed using a 62-day window, it might be useful to employ the high temporal resolution and investigate its use in forest fire research on impact monitoring and possibly active fire detection. For this, however, the effect of the processing window needs to be investigated and the window size would need to be minimized. Possibly even the daily measurements need to be used, rather than kernel-processed data. Considering this, the variables might have potential in short-term forest fire research, if adjusted to the purpose. On the other hand, the slope and curvature time series cover a long continuous period starting as early as 1991. This is interesting for forest fire recovery, as a forest might take several decades to recover and thus a long continuous time series would provide useful insights. The ASCAT variables thus have potential both in short-term and long-term forest fire analysis, but the potential needs to be further explored. Currently, the TUW SMR team is working on reprocessing the data to the higher spatial resolution of a 6km grid, which will improve the spatial abilities of the ASCAT variables as well, advancing the possibilities.

Another current limitation of the coarse spatial resolution is the physical interpretation of the time series. Although there are many sources on eucalyptus' post-forest fire behaviour, as well as specific field assessments after the Black Saturday Fires, it is difficult to relate these to the

ASCAT variables due to significantly different scales of the information. Additionally complicating the interpretation of the time series is that it is unknown how the post-fire behaviour looks in the microwave spectrum. For example, we understand the recovery in terms of epicormic resprouting and seed regeneration, but the difference in backscatter signal between the two recovery behaviours is unknown, due to which we are unable to interpret the slope and curvature signal in terms of these recovery behaviours. The information that was possible to dissect was the delayed response from the structural ASCAT variables compared to the NDVI signal, which indicated a recovery of canopy cover and greenness to the original levels more quickly than a structural recovery. This could however be the case for both epicormic resprouting and seedling regeneration; young shoots, both at ground level and as epicormic sprouts, can have similar NDVI as the original mature canopy.

Nonetheless, even if the scattering of those mechanisms was known, the problem remains that the forest is not homogeneous in forest type and in post-fire behaviour within the coverage of one ASCAT grid point. So currently the ASCAT variables are still troubled by both the heterogeneity of the response and the fact that it is unknown how those responses would look in the ASCAT variables. This is naturally a remote sensing problem, but it becomes less of a challenge with increasing spatial resolution.

Even though it remains speculative, this study attempted to relate the result to eucalyptus' post-fire behaviour as well as to other remote sensing studies of the same or similar fires. In general, the ASCAT variables showed results that were in line with other studies. The fact that the results could be related to other studies confirms the suitability of the ASCAT variables for vegetation research, as was for forest fire analysis. The feat that the ASCAT variables have a slower recovery signal than the NDVI could potentially be an interesting contribution to (multi-sensor) forest fire research, where structural recovery would be analysed separately from canopy recovery. It could for example be the case that the young regrowth has a similar NDVI to the original canopy, but physically still looks rather different. Structural investigation with the ASCAT variables could provive a more comprehensive insight in to how the canopy structurally looks.

With the current number of affected grid points, it was not possible to perform modelling or clustering efforts on the ASCAT variables. In a future study, it might be an option to look at global forest fire data and how it compares to the ASCAT variables, instead of focusing on one fire complex, to obtain more data points in space. For this effort, naturally, the soon-to-be-increased spatial resolution of the ASCAT variable will be of aid as well.

4.2. Fire severity, Z-score and Time Series Similarity

Within the results, it was determined that the Burn Scale did not influence the recovery timing. However, both the recovery in terms of Z-scores and the Burn Scale are parameters that can be considered ambiguous. The decision to work with the Burn Scale instead of a categorical fire severity like most studies has been explained in Section 2.3.1. However, this complicates comparing the results with other studies. It also is more challenging to explain the results in terms of fire severity. In future research, the role of fire severity and the use of a parameter such as the Burn Scale should be re-evaluated.

The Z-score was chosen to allow for the comparison of the different variables to each other in terms of magnitude. However, the Z-score is largely dependent on the standard deviation of the control grid points (see Equation 2.3). This causes any interpretation of the Z-scores to be heavily influenced by the size of this standard deviation, which for example differs greatly between the Dry Forest and Wet Forest points (with the Wet Forest generally having smaller standard deviations). If the control grid point were selected solely from the same vegetation class, these smaller standard deviations could be used to conclude that the Wet Forest is more homogeneous. However, the control grid points and thus the subsequent standard deviations are not selected based on vegetation class. In this case, a small standard deviation might cause a large deviation from

zero to appear, which is not an actual large difference in variable or vegetation, but just an exaggerated signal due to the small standard deviation. With the smaller standard deviations, magnitudes of impact and recovery might be overestimated and taken out of proportion.

The standard deviations are very dependent on the control grid points, which have been determined based on Time Series Similarity. This method is one of many methods to compare affected and unaffected grid points after a fire. An example of a temporal method is to compare an affected grid point after the fire to a moment in time before the fire. A potential spatial method is to compare the affected grid point to unaffected grid points with a similar vegetation class. This spatial method is rather similar to Time Series Similarity in processing but is troubled by within-class heterogeneity. These heterogeneities would be increasingly problematic with the coarse resolution of the ASCAT data. The Time Series Similarity approach that has been used in this study is based on the pixel-regeneration index (pRI) method by Lhermitte et al. (2010), which is a spatiotemporal control grid point selection approach. Additionally to the employed method, that method selects control grid points within a window, which increases in size until enough suitable control grid points are found. The spatial part of the method (i.e. the increasing window size) was not deemed necessary due to the scarce amount of grid points considered in this study. This, however, caused control grid points to be selected at vast distances from the affected grid point of interest. Grid points further away have a higher probability of showing different post-fire environmental conditions, such as different weather conditions (Lhermitte et al., 2010). This may have caused the control grid points to be a less suitable measure of 'what could have been, had nothing happened'.

The number of control grid points has been changed as well compared to Lhermitte et al. (2010) their method. The original method described the highest post-fire similarities obtained from VGT NDVI data when three to six control pixels are selected. In this study, nine control grid points have been used, which was necessary to control the exaggerations caused by very small standard deviations. Additionally, the magnitude of the ASCAT variables is of a different scale than those of the NDVI, it might therefore be that a different number of control grid points is ideal. The original method also did not utilise the Z-score, but a simpler $pRI = \frac{x}{\mu}$, where the standard deviation would simply not have caused a problem (x describes the affected grid point, μ the average of the control grid points). Although the reasoning for the Z-score was to be able to compare the different variables, the question arises whether the Z-score is suitable for such a time series similarity approach. Additionally, a time series similarity approach for change detection has not previously been used on the ASCAT variables. Although the pRI method is thought to be universal for different remote sensing derived time series of different kinds of sensors (Lhermitte et al., 2010), it is good to acknowledge the novel use of it for the ASCAT variables. In summary, the control grid point selection method and the use of the Z-score might not be a robust method, which will need to be addressed in future studies. For now, it is important to keep the control grid points and their influence on the Z-score in mind.

The challenges of the Z-score also influence the interpretation of the recovery. Recovery within the field of forest fire research is always a source of debate due to a lack of clarity in the definition of the term 'recovery' (Bartels et al., 2016). This lack of clarity exists on several levels, firstly, whether the grid point is only recovered when it reaches $Z = 0$ or can be considered recovered when it is close, or as mentioned before, when it is similar to the pre-fire Z-score. Secondly and more importantly, the question arises when a forest is recovered: Is recovery in terms of NDVI enough, as areas with young sprouts and a mature canopy can show the same NDVI value? Or is structural recovery as measured by the ASCAT variables required? Or might it be something else entirely? Different sources report vastly different things and it also depends on which ecosystem service is considered. For example, Benyon and Lane (2013) mention that the water quality and yield in the Victoria Eucalyptus forests remain affected by fire for up to 30 years. M. Tanase et al. (2011) describe that it takes decades for a forest to reach the biomass level, structure and carbon sink capacity of the forests pre-disturbance. On the contrary, Qin et al. (2022) state that the forest had recovered canopy cover and aboveground biomass 10 to 15 years after the Black Saturday Fires. Ultimately the question swivels back to what these remote

sensing parameters represent in the field, and thus that extensive ground-based validations are needed (Pérez-Cabello et al., 2021) before the ASCAT variables can be used as self-contained information sources in forest fire research. For such a ground-based validation study, it would be especially interesting to see how similar vegetation looks to the unaffected counterparts when the ASCAT variable Z-score indicates a recovered state. For the NDVI, it is known that both young vegetation and mature canopy can show the same NDVI values. For structural variables, this is less likely, but a discrepancy might still exist. Understanding this will aid the understanding of the ASCAT variables and their use in forest fire monitoring.

Nonetheless, for this study, it was determined that recovery is when Z-scores are zero. This results in the NDVI being mostly recovered by the end of the study period, and the ASCAT variables being generally close but not completely recovered. This corresponds to other studies and expectations that the leaves recover quicker than structural components (especially when considering epicormic resprouting). However, with the ambiguity of the Z-score, its recovery might be an artefact of the different standard deviations, resulting from different control grid points. This concern is reinforced by the actual time series in Appendix A which shows a clearer recovery of the ASCAT variables compared to pre-fire levels as well as to unaffected grid points of the same vegetation class. For a future study, it is advised to look at other parameters than the Z-score to determine recovery or use another control grid point selection method.

Although the method can be improved, the goal of this study was to identify whether the ASCAT variables are sensitive to forest fire and the consequent recovery and to gain qualitative insight into how the signal looks. This goal has been successfully achieved.

4.3. Microwaves and scattering mechanisms

The use of the ASCAT variables is based on the fire removing scatterers from the forest and scatterers growing back slowly over time. The backscatter signal of the forest is a complex interaction between microwave electromagnetic energy and the ground and vegetation scattering components (M. Tanase et al., 2011). However, the challenge of disentangling soil and vegetation effects remains (Steele-Dunne et al., 2019). With the improved slope σ' and curvature σ'', this disentanglement has been improved. With the TUW SMR, changes in soil moisture are described by backscatter σ^o, and surface roughness is assumed to be static. This means that the slope and curvature are less troubled by problems for example expressed by Fernandez-Carrillo et al. (2019), M. Tanase et al. (2011), and M. A. Tanase et al. (2015), where with the removal of vegetation scatterers the SAR backscatter becomes more sensitive to soil moisture. However, other challenges that are presented by the SAR investigation of fire severity and post-fire recovery remain challenges for the ASCAT variables as well. Examples are complex processing and analysis, decreased performance under wet conditions, and saturation that might occur over high aboveground biomass forests.

Additionally, problems have been mentioned with penetration through the canopy cover. Although M. Tanase et al. (2011) research investigates SAR microwaves, they found that PALSAR L-band was more sensitive to structural damages due to a fire disturbance as well as the subsequent recovery than ASAR C- and TerraSAR-X X-band waves. This sensitivity is due to L-band waves penetrating deeper through the canopy, making it more sensitive to the main trunks and branches, whereas C-band is thought to be more sensitive to smaller branches and leaves. Typically this would indeed be less adequate in measuring structural changes. However for eucalyptus forests, in most situations, the trunks do remain and only the minor branches and leaves are removed in high severity fires. For eucalyptus forests, C-band might therefore not be a bad choice. Besides that, several studies have described the suitability of ASCAT C-band waves for vegetation monitoring (Hahn et al., 2017; Pfeil et al., 2020; Steele-Dunne et al., 2019; Vreugdenhil et al., 2017; Wagner et al., 1999). The main take from the C-band — L-band discourse is that it is important to be careful in interpreting the slope and curvature variables until they are better understood.

4.4. Future directions

With this study, the eventual possibility to use the ASCAT variables for forest fire monitoring has been identified. However, there is still much to learn and understand. Firstly, it would be important to gain a better understanding of the slope σ' and curvature σ''.

Suggestions for future studies would firstly be to do a global forest fire investigation with the ASCAT variables, as the current spatial resolution lends itself better for this kind of investigation than for investigating a single fire complex. Such a study could provide an increased understanding of the interaction between forest fires and the ASCAT variables. A second suggestion focused more on the eucalyptus forest is to do a ground scatterometer study of the different recovery behaviours, such that these could be related to the coarser ASCAT signals and eventually be monitored with the ASCAT variables alone. Additionally to this suggestion is the fact that an unexpected counter phase between the slope and NDVI was found (see Appendix A), which should be investigated. Although it is known that NDVI and the ASCAT variables represent different physical processes, it is still phenologically unexpected because typically forests are healthy and green when they are filled with the most water. A dedicated study might be able to explain this, which will provide new insights into the understanding of slope. A ground study can also investigate whether grid points with a recovered slope and curvature signal appear to be physically similar to their unaffected counterparts in the field, or that similar slope and curvature can represent strikingly different canopy architectures.

Lastly, with the soon-to-be-increased spatial resolution, the long continuous time series, and the high temporal resolution, it is up to question whether the ASCAT variables are most suitable for short-term forest fire research or for long-term monitoring. Before the ASCAT variables could be adequately used in forest fire research, it should be investigated where it is most accomplished and if the data can be beneficial for forest fire research as they currently are, or needs to be processed differently for the application.

5

Conclusion

The goal of the study was to identify to what extent the ASCAT variables slope σ' and curvature σ'' respond to forest fires, both in terms of impact and recovery. Both variables show an impact and recovery over the following years after a major forest fire. The impact signal could be related to the removal of scatters by the fire and the recovery signal represent the regrowth of scatters in the vegetation. The variables are complementary to the commonly used forest fire index NDVI. The NDVI was used to validate and interpret the ASCAT variable signal. Both similarities and differences between the two variable types could be explained. In terms of recovery, a discrepancy between the NDVI and the structural ASCAT variables was found, which is thought to represent a slower structural recovery of a forest after a disturbance compared to the recovery of the leaves.

Nonetheless, there is still a lot to learn about the ASCAT variables and their interaction with post-forest fire behaviour. Especially a better understanding of the variables themselves, ground validation and increased spatial scale are needed to improve the suitability of these parameters for forest fire analysis.

There is potential in the ASCAT variables for forest fire analysis, and it is worth the time and effort to explore the opportunities further. Especially as the ASCAT variables will cover a long continuous period starting as early as 1991. This is interesting for forest fire recovery, as a forest might take several decades to recover and thus a long continuous time series is required. The ASCAT variables can be a useful addition to the multi-sensor analysis of post-forest fire due to their complementarity with NDVI. Such multi-sensor techniques are becoming an increasingly popular approach in forest fire monitoring (Chuvieco et al., 2020; M. A. Tanase et al., 2015). Contributing to the relevance of the ASCAT variables for forest fire research is the current effort to develop a 6km grid ASCAT product, greatly improving the current coarse resolution. Lastly, it is suggested that the ASCAT variables might be profitable in fire severity mapping due to the high temporal resolution and the clear impact that was seen in the variables. However, to do so a smaller temporal kernel width might be needed in processing the variables. Future research should identify whether the strength of the ASCAT variables is in the short-term forest fire research, or in long-term forest fire research.

References

Adams, M., & Attiwill, P. (2011). Ecology, fire and the Australian biota. In *Burning issues : Sustainability and management of australia's southern forests* (pp. 45–53). CSIRO Publishing.

Bartels, S. F., Chen, H. Y., Wulder, M. A., & White, J. C. (2016). Trends in post-disturbance recovery rates of canada's forests following wildfire and harvest. *Forest Ecology and Management*, *361*, 194–207. https://doi.org/https://doi.org/10.1016/j.foreco.2015.11.015

Bassett, M., Chia, E. K., Leonard, S. W., Nimmo, D. G., Holland, G. J., Ritchie, E. G., Clarke, M. F., & Bennett, A. F. (2015). The effects of topographic variation and the fire regime on coarse woody debris: Insights from a large wildfire. *Forest Ecology and Management*, *340*, 126–134. https://doi.org/10.1016/j.foreco.2014.12.028

Bennett, L. T., Bruce, M. J., Machunter, J., Kohout, M., Tanase, M. A., & Aponte, C. (2016). Mortality and recruitment of fire-tolerant eucalypts as influenced by wildfire severity and recent prescribed fire. *Forest Ecology and Management*, *380*, 107–117. https://doi.org/10.1016/j.foreco.2016.08.047

Benyon, R. G., & Lane, P. N. (2013). Ground and satellite-based assessments of wet eucalypt forest survival and regeneration for predicting long-term hydrological responses to a large wildfire. *Forest Ecology and Management*, *294*, 197–207. https://doi.org/10.1016/j.foreco.2012.04.003

Bond, W. J., Woodward, F. I., & Midgley, G. F. (2005). The global distribution of ecosystems in a world without fire. *New phytologist*, *165*(2), 525–538.

Bureau of Meteorology. (2016). Climate classification maps. Retrieved February 15, 2022, from http://www.bom.gov.au/jsp/ncc/climate_averages/climate-classifications/index.jsp?maptype=tmp_zones#maps

Chuvieco, E., Aguado, I., Salas, J., García, M., Yebra, M., & Oliva, P. (2020). Satellite Remote Sensing Contributions to Wildland Fire Science and Management Introduction : Why Using RS Methods in Fire. *Current Forestry Reports*, *6*, 81–96. https://doi.org/https://doi.org/10.1007/s40725-020-00116-5FIRE

Cruz, M. G., Sullivan, A. L., Gould, J. S., Sims, N. C., Bannister, A. J., Hollis, J. J., & Hurley, R. J. (2012). Anatomy of a catastrophic wildfire: The Black Saturday Kilmore East fire in Victoria, Australia. *Forest Ecology and Management*, *284*, 269–285. https://doi.org/10.1016/j.foreco.2012.02.035

Department of Environment, Land, Water and Planning. (2018a). *Native vegetation - modelled 2005 ecological vegetation classes (with bioregional conservation status)* (Version 29-11-2021). DataVic. https://discover.data.vic.gov.au/dataset/native-vegetation-modelled-2005-ecological-vegetation-classes-with-bioregional-conservation-sta

Department of Environment, Land, Water and Planning. (2018b). *Victorian bushfires severity map 2009 (polygons)* (Version 22-06-2022). DataVic. https://metashare.maps.vic.gov.au/geonetwork/srv/api/records/c0559b38-c8b7-5f05-89ca-02c878345c1d/formatters/sdm-html?root=html&output=html

Didan, K. (2021). *MODIS/Terra vegetation indices 16-day L3 global 250m SIN grid V061*. NASA EOSDIS Land Processes DAAC. https://developers.google.com/earth-engine/datasets/catalog/MODIS_061_MOD13Q1#description

Fairman, T. A., Nitschke, C. R., & Bennett, L. T. (2016). Too much, too soon? A review of the effects of increasing wildfire frequency on tree mortality and regeneration in temperate eucalypt forests. *International Journal of Wildland Fire*, *25*(8), 831–848. https://doi.org/10.1071/WF15010

Fernandez-Carrillo, A., Mccaw, L., & Tanase, M. A. (2019). Estimating prescribed fire impacts and postfire tree survival in eucalyptus forests of Western Australia with L-band SAR data. *Remote Sensing of Environment*, *224*(September 2018), 133–144. https://doi.org/10.1016/j.rse.2019.02.005

Gill, A. (1981). Adaptive responses of australian vascular plant species to fires. In *Fire and the australian biota*. Australian Academy of Science.

Gullan, P. (2008a). Damp Sclerophyll Forest. Retrieved November 22, 2022, from http://www.viridans.com/ECOVEG/damp%20sclerophyll.htm

Gullan, P. (2008b). Dry Sclerophyll Forest. Retrieved November 22, 2022, from http://www.viridans.com/ECOVEG/dry%20sclerophyll.htm

Gullan, P. (2008c). Wet Sclerophyll Forest. Retrieved November 22, 2022, from http://www.viridans.com/ECOVEG/wet%20sclerophyll.htm

Hahn, S., Reimer, C., Vreugdenhil, M., Melzer, T., & Wagner, W. (2017). Dynamic Characterization of the Incidence Angle Dependence of Backscatter Using Metop ASCAT. *IEEE Journal of Selected Topics in Applied Earth Observations and Remote Sensing*, *10*(5), 2348–2359. https://doi.org/10.1109/JSTARS.2016.2628523

Heath, J. T., Chafer, C. J., Bishop, T. F., & van Ogtrop, F. F. (2016). Post-fire recovery of eucalypt-dominated vegetation communities in the sydney basin, Australia. *Fire Ecology*, *12*(3), 53–79. https://doi.org/10.4996/fireecology.1203053

João, T., João, G., Bruno, M., & João, H. (2018). Indicator-based assessment of post- fi re recovery dynamics using satellite. *Ecological Indicators*, *89*(February), 199–212. https://doi.org/10.1016/j.ecolind.2018.02.008

Karna, Y. K., Penman, T. D., Aponte, C., Hinko-najera, N., & Bennett, L. T. (2020). Persistent changes in the horizontal and vertical canopy structure of fire-tolerant forests after severe fire as quantified using multi-temporal airborne lidar data. *Forest Ecology and Management*, *472*(April), 118255. https://doi.org/10.1016/j.foreco.2020.118255

Keith, H., Lindenmayer, D. B., MacKey, B. G., Blair, D., Carter, L., McBurney, L., Okada, S., & Konishi-Nagano, T. (2014). Accounting for biomass carbon stock change due to wildfire in temperate forest landscapes in Australia. *PLoS ONE*, *9*(9). https://doi.org/10.1371/journal.pone.0107126

Lentile, L. B., Morgan, P., Hudak, A. T., Bobbitt, M. J., Lewis, S. A., Smith, A. M., & Robichaud, P. R. (2007). Post-Fire Burn Severity and Vegetation Response Following Eight Large Wildfires Across The Western United States. *Fire Ecology*, *3*(1), 91–108.

Leonard, S. W., Bennett, A. F., & Clarke, M. F. (2014). Determinants of the occurrence of unburnt forest patches: Potential biotic refuges within a large, intense wildfire in south-eastern Australia. *Forest Ecology and Management*, *314*, 85–93. https://doi.org/10.1016/j.foreco.2013.11.036

Lhermitte, S., Verbesselt, J., Verstraeten, W. W., Veraverbeke, S., & Coppin, P. (2011). Assessing intra-annual vegetation regrowth after fire using the pixel based regeneration index. *ISPRS Journal of Photogrammetry and Remote Sensing*, *66*(1), 17–27. https://doi.org/10.1016/j.isprsjprs.2010.08.004

Lhermitte, S., Verbesselt, J., Verstraeten, W. W., & Coppin, P. (2010). A Pixel Based Regeneration Index using Time Series Similarity and Spatial Context. *Photogrammetric Engineering & Remote Sensing*, *76*(6), 673–682.

Massetti, A., Rüdiger, C., Yebra, M., & Hilton, J. (2019). The Vegetation Structure Perpendicular Index (VSPI): A forest condition index for wildfire predictions. *Remote Sensing of Environment*, *224*(November 2017), 167–181. https://doi.org/10.1016/j.rse.2019.02.004

McCaw, W. L., Smith, R. H., & Neal, J. E. (1994). Stem damage and crown recovery following high intensity fire in a 16-year-old stand of Eucalyptus diversicolor and Eucalyptus muellerana. *Australian Forestry*, *57*(2), 76–81. https://doi.org/10.1080/00049158.1994.10676118

Melzer, T. (2013). Vegetation Modelling in WARP 6.0. *Proc. EUMETSAT Meteorological Satellite Conf., Vienna*, 1–7.

Naeimi, V., Scipal, K., Bartalis, Z., Hasenauer, S., Wagner, W., & Member, S. (2009). An Improved Soil Moisture Retrieval Algorithm for ERS and METOP Scatterometer Observations. *IEEE Transactions on Geoscience and Remote Sensing*. https://doi.org/10.1109/TGRS.2008.2011617

Paulik, C., Preimesberger, W., s-scherrer, pstradio, Hahn, S., Baum, D., Plocon, A., Mistelbauer, T., teije01, tracyscanlon, Schmitzer, M., alegrub88, & iteubner. (2022). *Tuw-geo/pytesmo: V0.13.3* (Version v0.13.3). Zenodo. https://doi.org/10.5281/zenodo.5837443

Pérez-Cabello, F., Montorio, R., & Alves, D. B. (2021). Remote sensing techniques to assess post-fire vegetation recovery. *Current Opinion in Environmental Science & Health*, *21*, 100251. https://doi.org/10.1016/j.coesh.2021.100251

Petchiappan, A., Steele-Dunne, S., Vreugdenhil, M., Hahn, S., Wagner, W., & Oliveira, R. (2022). The influence of vegetation water dynamics on the ASCAT backscatter-incidence angle relationship in the Amazon. *Hydrology and Earth System Sciences*, *26*(11), 2997–3019. https://doi.org/https://doi.org/10.5194/hess-26-2997-2022

Pfeil, I., Wagner, W., Forkel, M., Dorigo, W., & Vreugdenhil, M. (2020). Does ASCAT observe the spring reactivation in temperate deciduous broadleaf forests? *Remote Sensing of Environment*, *250*(August), 112042. https://doi.org/10.1016/j.rse.2020.112042

Polychronaki, A. (2014). Monitoring post-fire vegetation recovery in the Mediterranean using SPOT and ERS imagery. *International Journal of Wildland Fire*, *23*, 631–642.

Qin, Y., Xiao, X., Wigneron, J. P., Ciais, P., Canadell, J. G., Brandt, M., Li, X., Fan, L., Wu, X., Tang, H., Dubayah, R., Doughty, R., Crowell, S., Zheng, B., & Moore, B. (2022). Large loss and rapid recovery of vegetation cover and aboveground biomass over forest areas in Australia during 2019–2020. *Remote Sensing of Environment*, *278*(October 2021), 113087. https://doi.org/10.1016/j.rse.2022.113087

Steele-Dunne, S. C., Hahn, S., Wagner, W., & Vreugdenhil, M. (2019). Investigating vegetation water dynamics and drought using Metop ASCAT over the North American Grasslands. *Remote Sensing of Environment*, *224*(January), 219–235. https://doi.org/10.1016/j.rse.2019.01.004

Steele-Dunne, S. C., Hahn, S., Wagner, W., & Vreugdenhil, M. (2021). Towards Including Dynamic Vegetation Parameters in the EUMETSAT H SAF ASCAT Soil Moisture Products. *Remote Sensing*, *13*(1463), 1–16. https://doi.org/https://doi.org/10.3390/rs13081463Academic

Tanase, M., de la Riva, J., Santoro, M., Pérez-Cabello, F., & Kasischke, E. (2011). Sensitivity of SAR data to post-fire forest regrowth in Mediterranean and boreal forests. *Remote Sensing of Environment*, *115*(8), 2075–2085. https://doi.org/10.1016/j.rse.2011.04.009

Tanase, M., Kennedy, R., & Aponte, C. (2015). Radar Burn Ratio for fire severity estimation at canopy level: An example for temperate forests. *Remote Sensing of Environment*, *170*, 14–31. https://doi.org/10.1016/j.rse.2015.08.025

Tanase, M., Santoro, M., de la Riva, J., Kasischke, E., & Korets, M. A. (2010). L-band sar backscatter prospects for burn severity estimation in boreal forests. *Proc. ESA Living Planet Symp*.

Tanase, M. A., Kennedy, R. E., & Aponte, C. (2015). Fire severity estimation from space: A comparison of active and passive sensors and their synergy for different forest types. *Internation Journal of Wildland Fire*, (June).

Tanase, M. A., Panciera, R., Lowell, K., Tian, S., Garcia-Martin, A., & Walker, J. P. (2013). Sensitivity of l-band radar backscatter to forest biomass in semiarid environments: A comparative analysis of parametric and nonparametric models. *IEEE Transactions on Geoscience and Remote Sensing*, *52*(8), 4671–4685.

Turner, M. G., Baker, W. L., Peterson, C. J., & Peet, R. K. (1998). Factors influencing succession: Lessons from large, infrequent natural disturbances. *Ecosystems*, *1*(6), 511–523.

Veraverbeke, S., Gitas, I., Katagis, T., Polychronaki, A., Somers, B., & Goossens, R. (2012). Assessing post-fire vegetation recovery using red-near infrared vegetation indices: Accounting for background and vegetation variability. *ISPRS Journal of Photogrammetry and Remote Sensing*, *68*(1), 28–39. https://doi.org/10.1016/j.isprsjprs.2011.12.007

Vivian, L. M., Doherty, M. D., & Cary, G. J. (2010). Classifying the fire-response traits of plants: How reliable are species-level classifications? *Austral Ecology*, *35*(3), 264–273. https://doi.org/10.1111/j.1442-9993.2009.02032.x

Vreugdenhil, M., Hahn, S., Melzer, T., Bauer-marschallinger, B., Reimer, C., Dorigo, W. A., Wagner, W., & Member, S. (2017). Assessing Vegetation Dynamics over Mainland Australia With Metop ASCAT. *10*(5), 2240–2248.

Wagner, W., Lemoine, G., Borgeaud, M., Member, S., & Rott, H. (1999). A Study of Vegetation Cover Effects on ERS Scatterometer Data. *IEEE Transactions on Geoscience and Remote Sensing*, *37*(2), 938–948.

Walraven, B. (2021). *Monitoring the impact of droughts on vegetation in Australia using MetOp ASCAT Dynamic Vegetation Parameters*. https://repository.tudelft.nl/islandora/object/uuid%5C%3Ae3b56111-7911-4854-a759-87e5f45db118?collection=education

A

Individual Time Series

In this chapter, the individual time series for the 13 affected grid points are shown for all three variables. They are presented against a 20th — 80th quantile range of unaffected grid points. For this range, grid points of the corresponding vegetation class are used. Note, that these are not the same as the control grid point used in the analysis. For more information on the control grid points, see Appendix B.

The affected grid points are selected as described in Chapter 2. The unaffected grid point used for the range here are selected according to the rule below. The results are 40 Dry Forest unaffected grid points, and eight Wet Forest unaffected grid points.

- **Dry Forest Unaffected grid points**: 'FS1 + FS2 + FS3 + FS4 + FS5' < 50% & FS1 < 2% & Dry Forest > 65%
- **Wet Forest Unaffected grid points**: 'FS1 + FS2 + FS3 + FS4 + FS5' < 50% & FS1 < 2% & Wet Forest > 65%

The individual time series are presented in Figure A.1 up to Figure A.6.

A.1. Slope

The slope time series present a clear seasonal cycle for both the Dry and Wet Forest. This seasonal cycle has a larger amplitude in the Dry Forest. After the fire, the seasonal cycle is somewhat subdued, especially in the Wet Forest. This is seen both in the affected time series, as well as in the unaffected range. This subdued seasonal cycle can likely be explained by above average rainfall in 2010 and 2011. After 2012, the seasonal cycle restores to pre-fire levels. The seasonal cycle shows a peak in SH Summer, which means that in Summer there is more volume scattering than in SH Winter.

The unaffected range of the Wet Forest is smaller than that of the Dry Forest, which might imply that the Wet Forest is more homogeneous. However this is not certain as the number of selected unaffected grid points is small compared to those for Dry Forest. In the Wet Forest, the slope is generally slightly higher than in the Dry Forest, which is most likely a result of the higher moisture content in the Wet Forest, as well as the denser vegetation.

In most slope time series, we see a clear negative deviation (or impact) shortly after the fire. Whether this effect is clearly visible corresponds in the most part with the % and severity of the area burned. Interestingly. the unaffected range shows a deviation from its typical levels in 2009 as (especially in the Wet Forest). This can be explained by unaffected grid points containing burned areas, as well as by the fact that the extreme fire weather that created the Black Saturday Fires also impacted the unaffected vegetation in terms of drought, having the same effect on the slope variable.

A.2. Curvature

The curvature time series do not show a clear seasonality. The curvature time series show a clear positive deviation shortly after the fire, where the curvature largely increases for some time before returning to pre-fire levels. Just like the slope, the impact seems to be somewhat related to the fire severity distribution and the % burned. The Dry Forest appears to have slightly higher curvature values than the Wet Forest. What causes this is unclear.

The unaffected range of the curvature is larger for the Dry Forest than for the Wet Forest, which once again might indicate a higher homogeneity for the Wet Forest, but could also be due to the smaller number of unaffected grid points. For the Wet Forest, the unaffected range also has a small increase after the fire, similar to what was seen in the slope. In the Dry Forest this effect is less clear, however, the Dry Forest unaffected range is situated closer to zero post-fire than pre-fire. Thus the period of forest fires seems to have influenced the unaffected Dry Forest grid points as well.

A.3. NDVI

The NDVI time series (and unaffected ranges) show a seasonality, which is more distinct in the Dry Forest than in the Wet Forest, where the seasonality only has a very small amplitude. In the year 2011, the seasonality is not present (in both affected and unaffected grid points), most likely due to the exceptionally wet year. The NDVI is lowest in SH Summer and highest in SH Winter, meaning that it is in counter-phase with the slope, which is unexpected. NDVI is probably highest in SH Winter due to Eucalyptus favouring wet growing conditions, which occur in Winter. However, one would expect that favourable growing conditions would result in higher slope as well, which is not the case. What causes this counter-phase is therefore unknown, and interesting for future studies, where for example one could look at other vegetation types as well. An interesting note might also be that the slope (and curvature) react to vegetation water content, but that Eucalyptus also contains oil in the leaves. The effect of this oil on slope and curvature is unknown, and could be food for thought as well.

The unaffected range of the NDVI Dry Forest is broader than for the Wet forest, for the same reasons as with the slope and curvature. Nonetheless, the Dry Forest range shows a large range in SH Summer, and a very small range in SH Winter. This means that in Summer there are large differences between the greenness of the Dry Forest, whereas in Winter everything is very homogeneous. This effect is not seen in the Wet Forest.

Most of the affected grid point time series show a clear and immediate response to the fire. After this the seasonality is lost for some years. The same pattern is seen as in the slope and curvature, where the impact seems to be mostly related to the fire severity distribution and the % affected. For the NDVI, it becomes also apparent that if only slightly over 50% is burned, or only little high fire severities occur, that the impact is really small or non-existent compared to NDVI impact of more affected grid points. This difference was less clear in the slope and curvature.

A.4. Individual Time Series

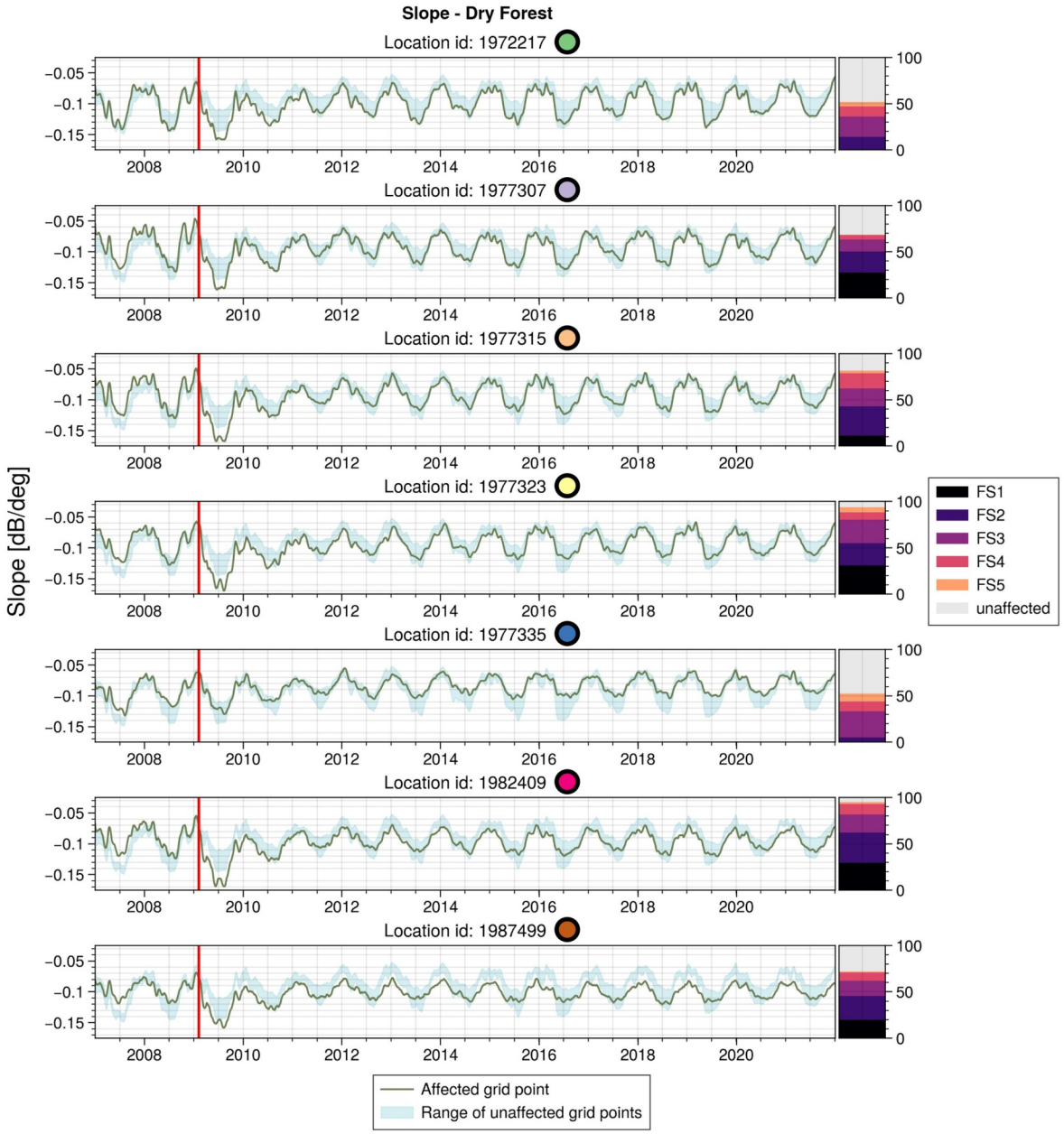

Figure A.1

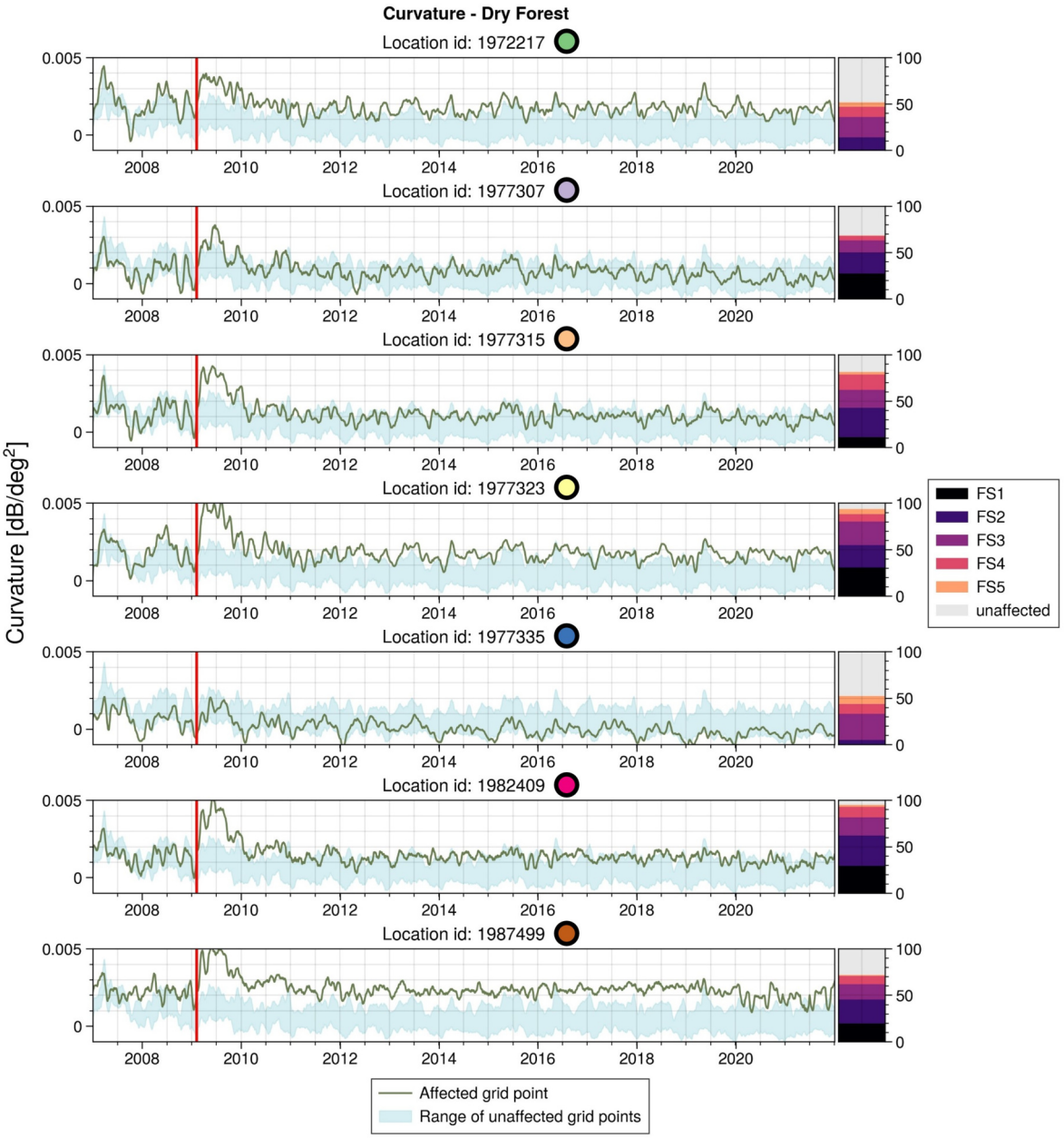
Curvature - Dry Forest
Location id: 1972217
Location id: 1977307
Location id: 1977315
Location id: 1977323
Location id: 1977335
Location id: 1982409
Location id: 1987499
Curvature [dB/deg²]
0.005
0
2008
2010
2012
2014
2016
2018
2020
100
50
0
FS1
FS2
FS3
FS4
FS5
unaffected
Affected grid point
Range of unaffected grid points

Figure A.2

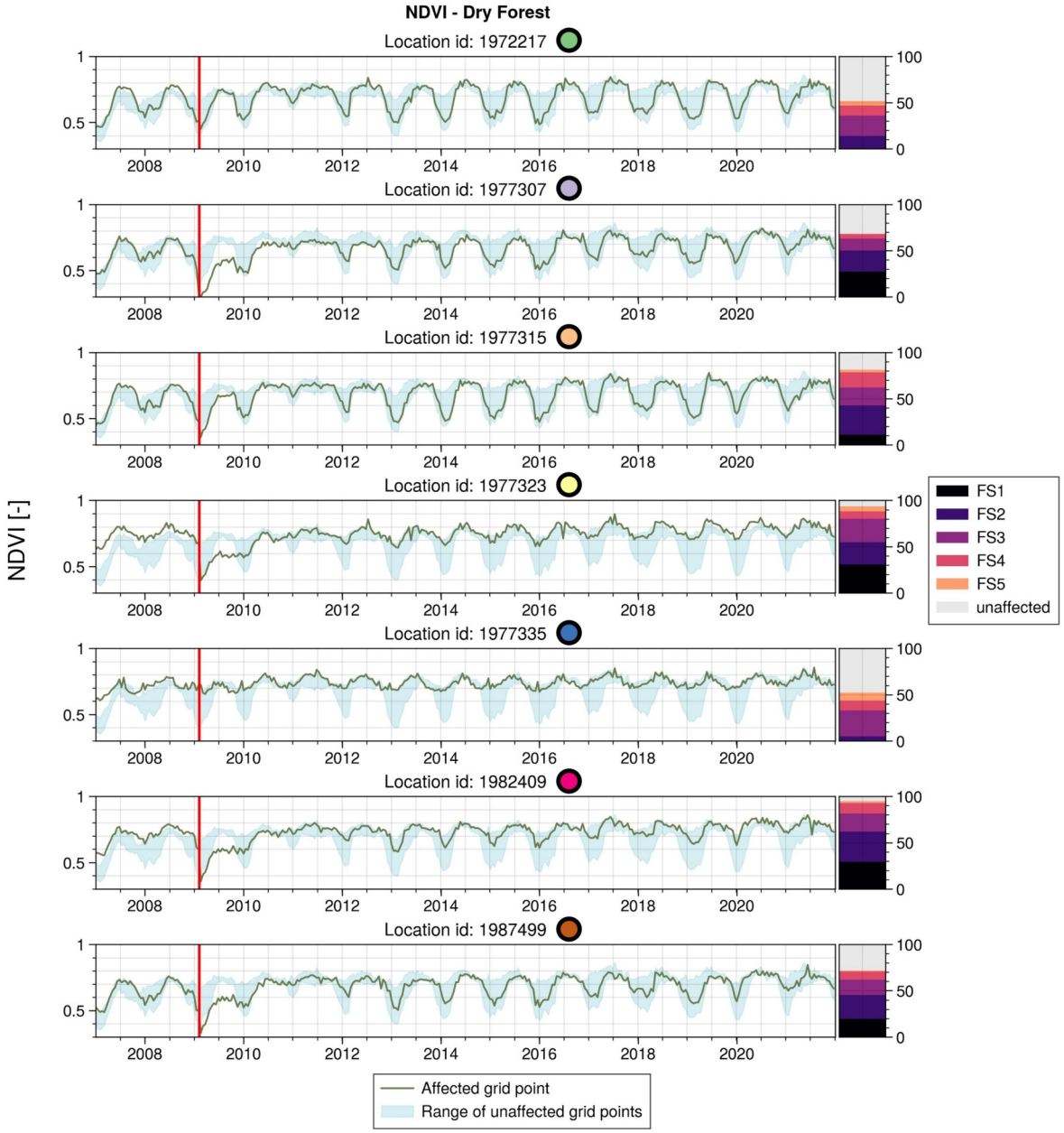
NDVI - Dry Forest
Location id: 1972217
Location id: 1977307
Location id: 1977315
Location id: 1977323
Location id: 1977335
Location id: 1982409
Location id: 1987499
NDVI [-]
1
0.5
2008
2010
2012
2014
2016
2018
2020
100
50
0
FS1
FS2
FS3
FS4
FS5
unaffected
Affected grid point
Range of unaffected grid points

Figure A.3

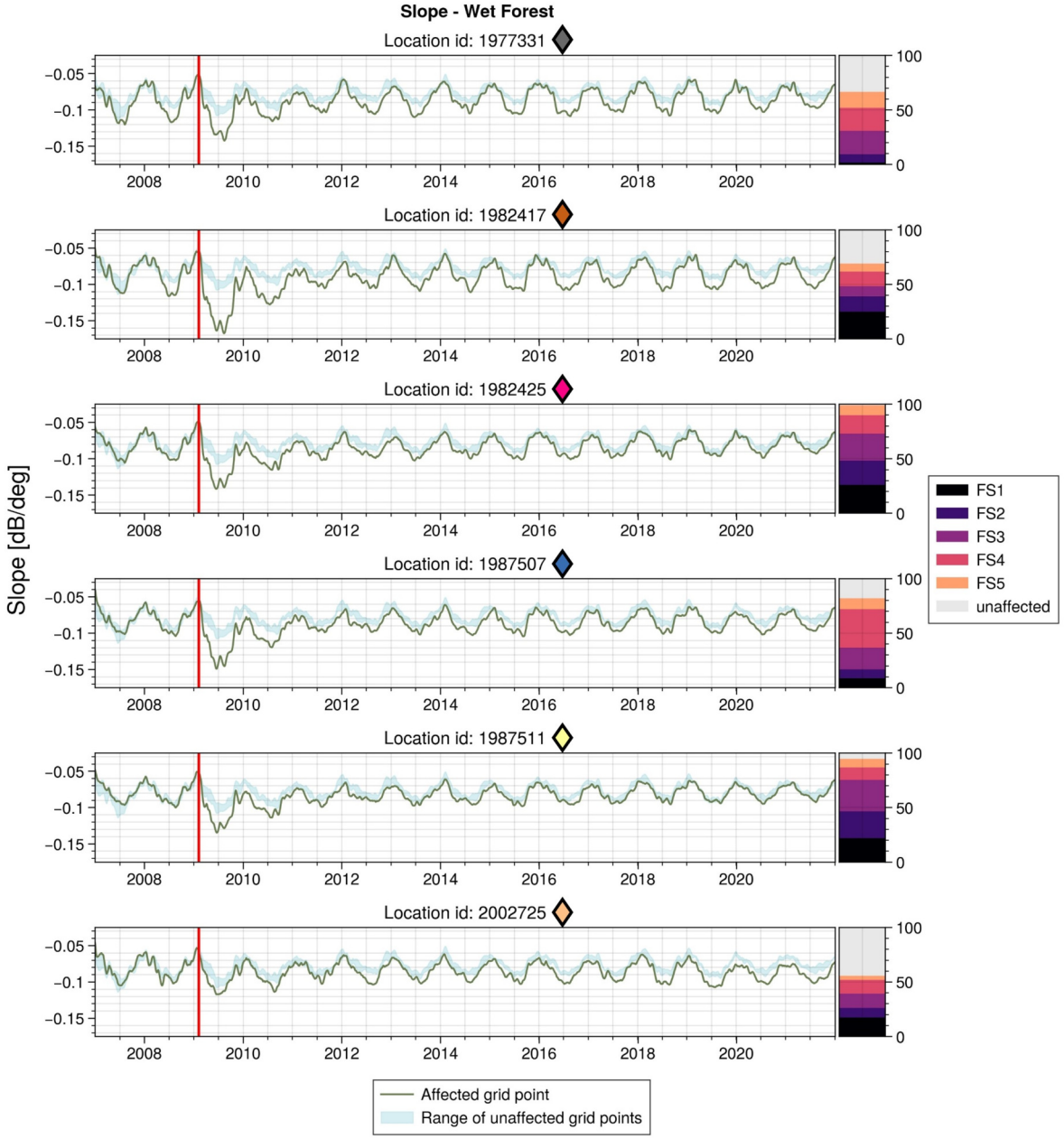
Slope - Wet Forest
Location id: 1977331
Location id: 1982417
Location id: 1982425
Location id: 1987507
Location id: 1987511
Location id: 2002725
Slope [dB/deg]
−0.05
−0.1
−0.15
2008
2010
2012
2014
2016
2018
2020
100
50
0
FS1
FS2
FS3
FS4
FS5
unaffected
Affected grid point
Range of unaffected grid points

Figure A.4

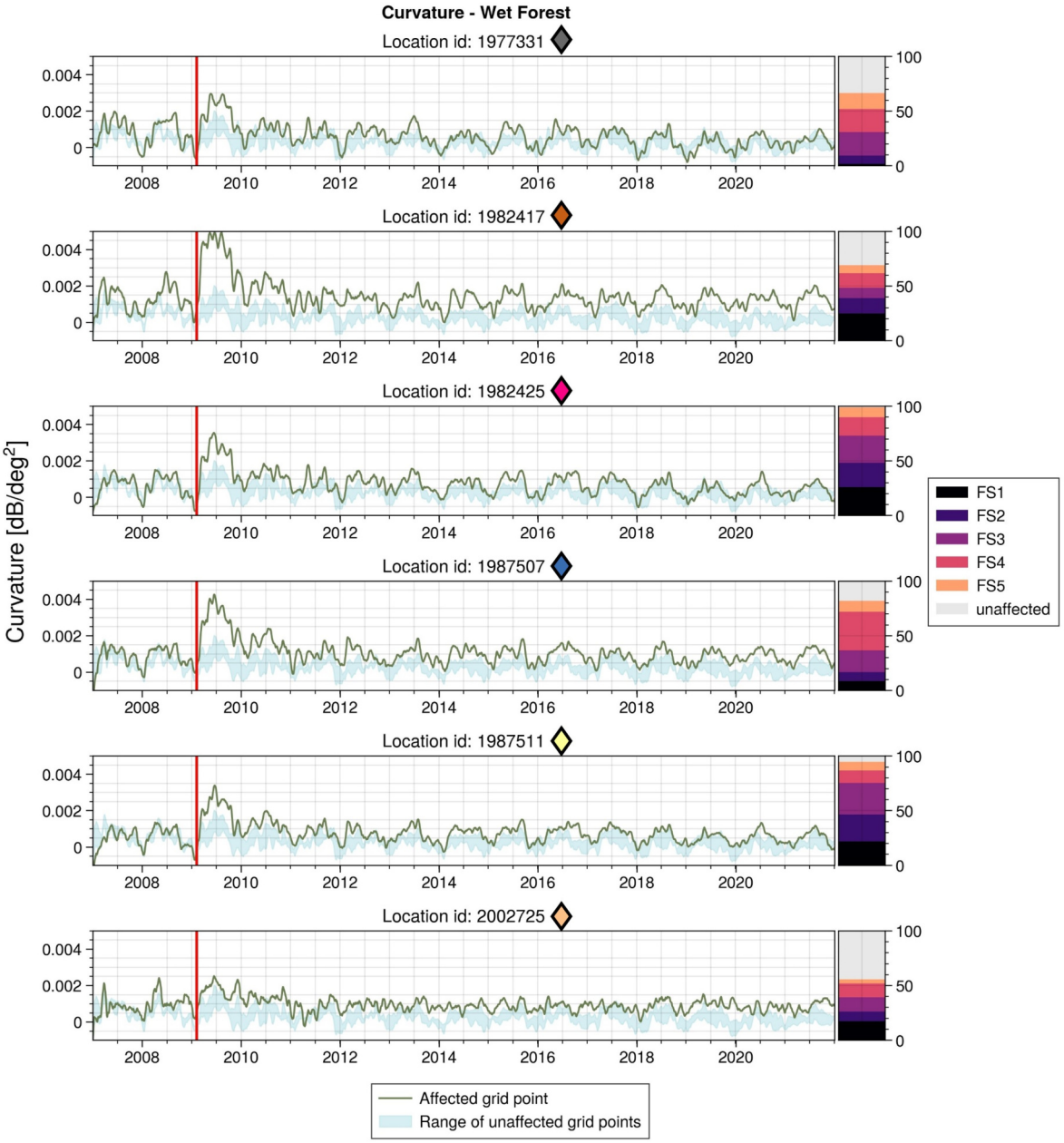
Curvature - Wet Forest
Location id: 1977331
Location id: 1982417
Location id: 1982425
Location id: 1987507
Location id: 1987511
Location id: 2002725
Curvature [dB/deg²]
0.004
0.002
0
2008
2010
2012
2014
2016
2018
2020
100
50
0
FS1
FS2
FS3
FS4
FS5
unaffected
Affected grid point
Range of unaffected grid points

Figure A.5

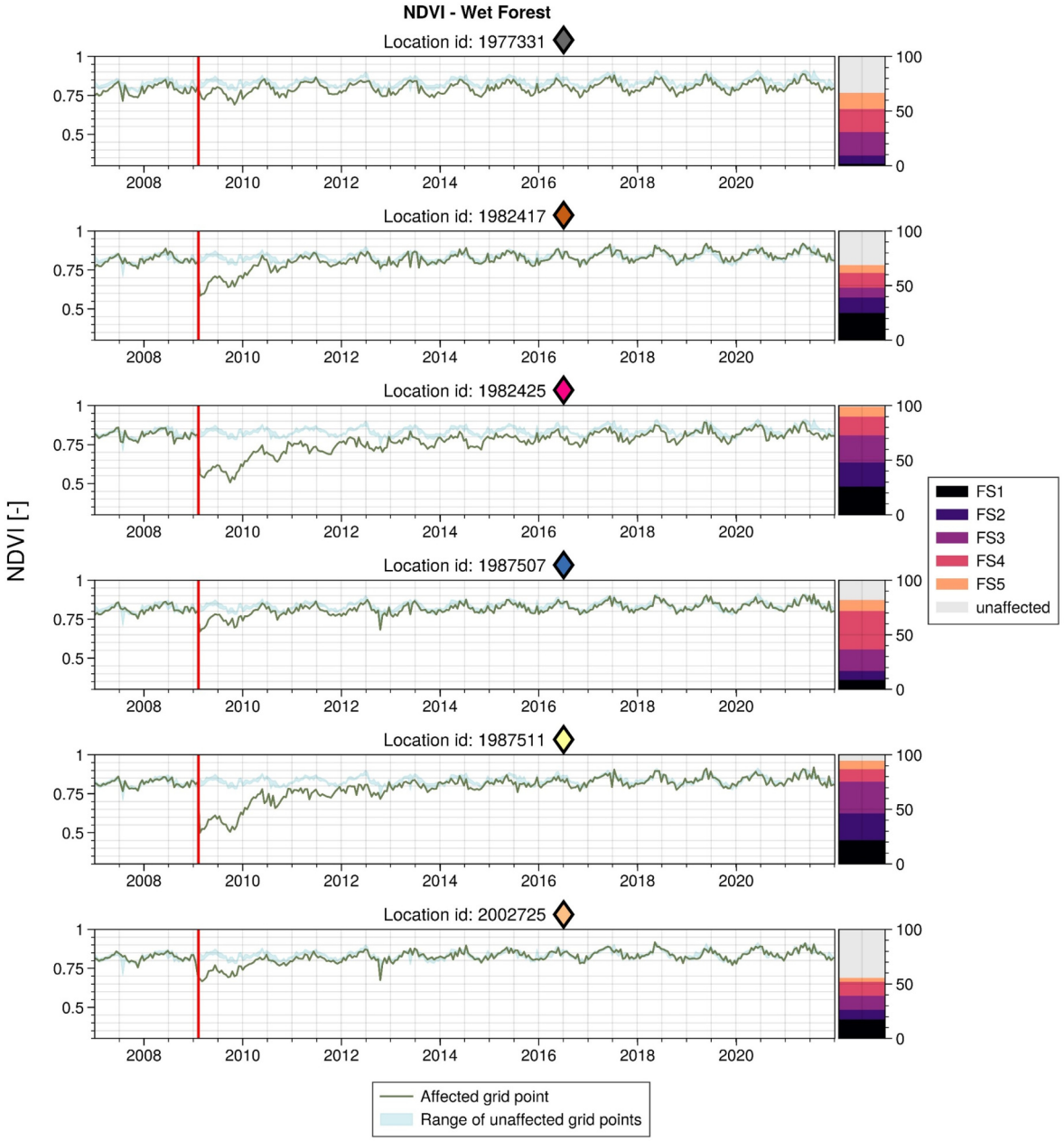
NDVI - Wet Forest
Location id: 1977331
Location id: 1982417
Location id: 1982425
Location id: 1987507
Location id: 1987511
Location id: 2002725
NDVI [-]
1
0.75
0.5
2008
2010
2012
2014
2016
2018
2020
100
50
0
FS1
FS2
FS3
FS4
FS5
unaffected
Affected grid point
Range of unaffected grid points

Figure A.6

B

Control Grid Point Selection

As discussed in Chapter 2, the control grid point selection is solely based on the smallest RMSD values between the affected focal grid point and the unaffected grid points in the two years prior the fire. For these RMSDs no cut-off value is used, nor a selection based on vegetation class. For each variable, the control gridpoints have been determined seperately, this appendix will also investigate whether the control gridpoints for the different variables are similar.

B.1. No Cut-Off Value

Lhermitte et al. (2010) introduced a cut-off value because they worked with an increasing window size until 'the best fits' were found as control grid points. The cut-off value of RMSD < 0.2 for NDVI values was used to ensure that the control grid points indeed showed 'what would have been, had the fire not occurred'. However, the increasing window size was not necessary in the scale of our study: the ASCAT grid points (and thus the resampled NDVI) have such a low spatial resolution, that it was computationally viable to compare the affected grid point to all available unaffected grid points in the study area. From all these available unaffected grid points, the nine with the smallest RMSD have been chosen.

Nonetheless, it is interesting to see whether the selected RMSDs are within an acceptable range. Therefore, for each affected grid points the median RMSD of the selected control grid point has been determined. These averages have been compared to histograms of all RMSD values to determine whether they are indeed within acceptable range compared to all other RMSD values of the unchosen unaffected gridpoints. These results are shown in Figure B.1. The figure shows that all selected RMSD medians are below the NDVI cut-off, and likely this also translates to the other variables.

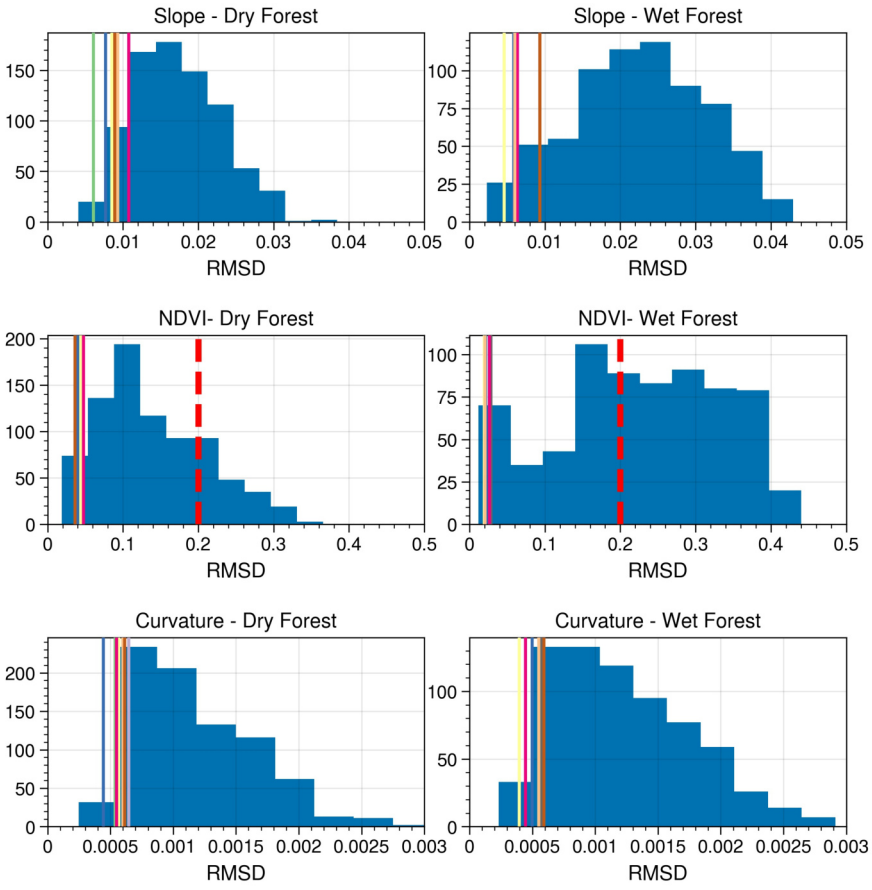

Figure B.1: Histograms presenting all RMSD values between affected grid points and unaffected grid points. Vertical lines represent the median RMSD of the selected control grid points for each affected gridpoint. The dashed vertical line in the NDVI diagrams represent the cut-off value used by Lhermitte et al. (2010).

B.2. Control Grid point Similarity between variables

As the control grid points are determined separately for each grid point and for each variable, there is a possibility that there is a difference in which unaffected gridpoints are chosen. Figure B.2 shows an example of how for the same focal grid point, different control grid points have been chosen for each variable. Further investigation showed that this is the case for all affected grid points.

The question arises whether the choices were 'close calls', i.e. the control grid points chosen for one variable were close to being selected for another variable. To investigate this the RMSDs of the control grid point selected by one variable are compared to the RMSDs of the control grid-points selected by all variables. So for example, for a focal grid point, we compare the RMSDs of the slope control grid points to the slope RMSDs of the control grid points selected based on slope, curvature and NDVI. The results are shown in the boxplots of Figure B.3. From these figures, it becomes clear that the grid points selected for each variable are significantly different from the grid points selected for the other grid points. With that, the choice to separate the control grid point selection has been justified.

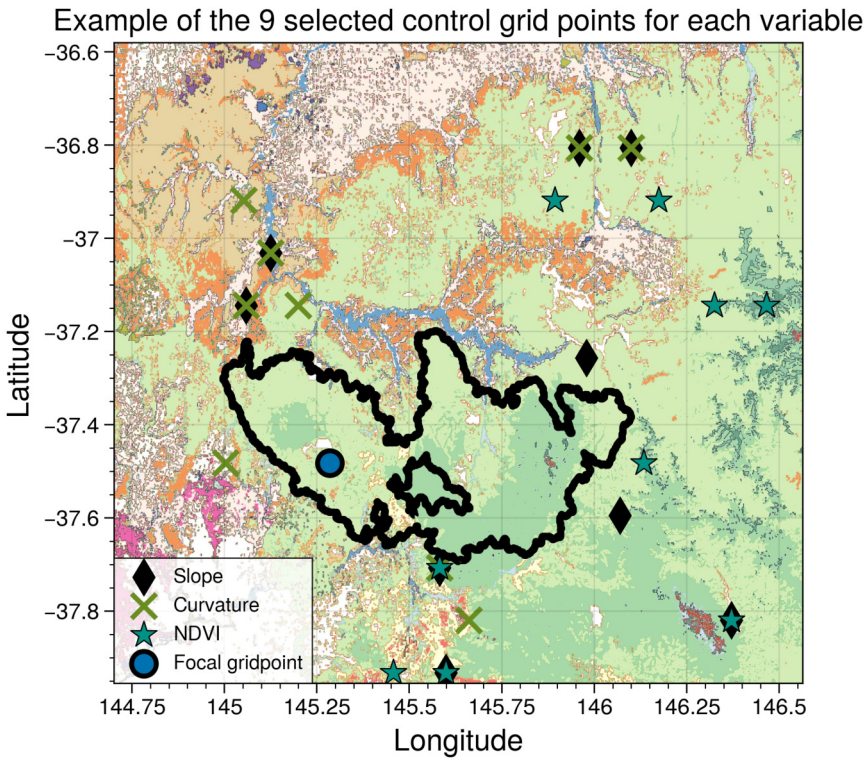

Figure B.2: Example of an affected grid point and the difference between selected control grid points for different variables

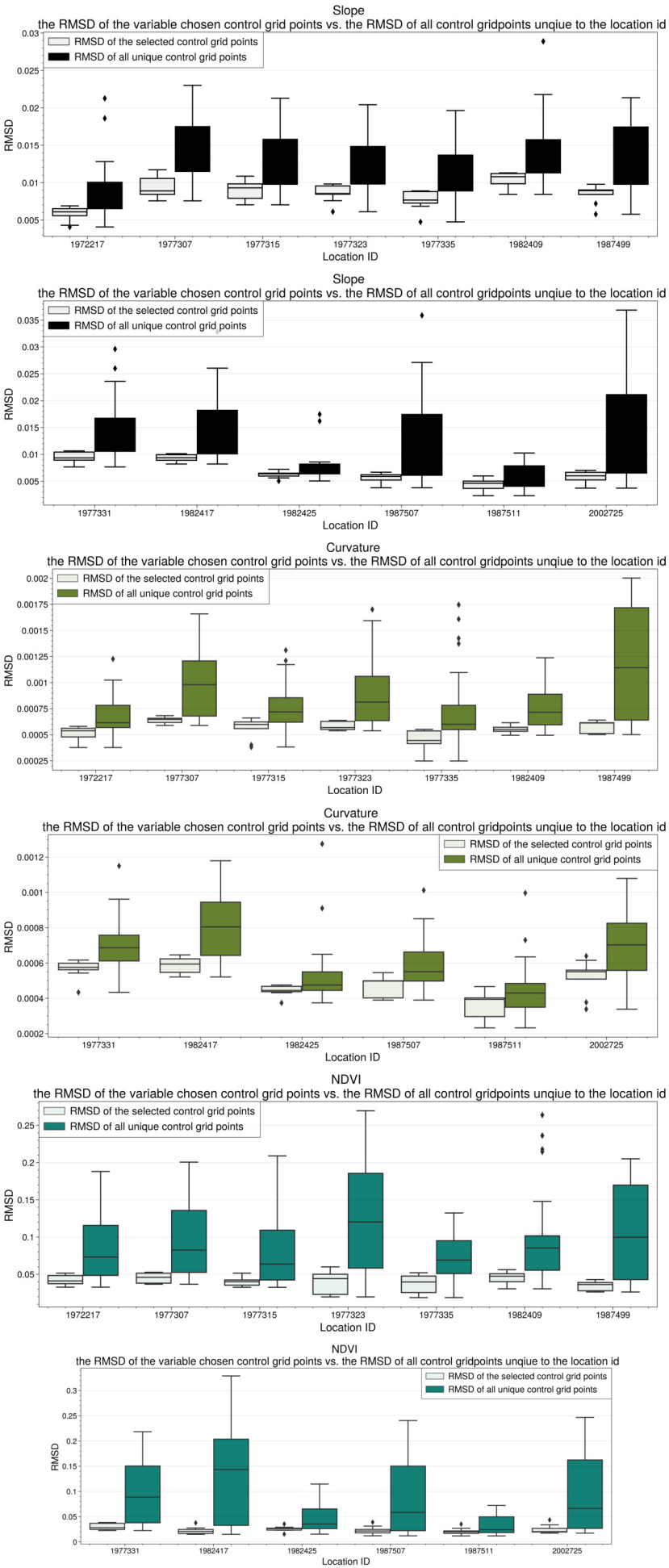

Figure B.3: For each variable, the nine control grid points are selected separately. The figure shows different control grid points being selected for the different variables. It also is apparent that the selected control grid points are situated in different vegetation classes than the affected grid point.

B.3. Control grid point vegetation classes

In Figure 2.9 and Figure B.2 it already became apparent that the selected control grid points are not necessarily within the same vegetation class as the focal grid point. To further investigate this, the vegetation classes of the selected control grid points are compared to the vegetation class of the focal grid point, both visually (an example is provided in Figure B.4) as well as by means of cosine similarity. Cosine similarity is typically used to determine how alike texts are, but for this application it determines on a scale from 0-1 how similar the vegetation class distribution is, where one represents identical and zero represents no similarity. For each focal grid point, the cosine similarities with their control grid points are averaged (median), the results are presented in Figure B.5.

From the cosine similarities, we see that quite often the similarity is high (>0.9), especially in the Dry Forest. In the Wet Forest, we see generally smaller similarities between the focal grid points vegetation class and its control grid points. For the different variables, there does not seem to be a striking difference between which variable produces more similar control grid points. Looking at Table B.1, we see that for the NDVI on average control grid points are selected with worse matching vegetation classes than for the slope and curvature. The slope also has worse matches on average than the curvature. There is no clear explanation as to why this would be the case.

Table B.1: Mean cosine similarities for each variable

	Dry Forest	Wet Forest
Slope	0.94	0.91
Curvature	0.98	0.99
NDVI	0.87	0.81

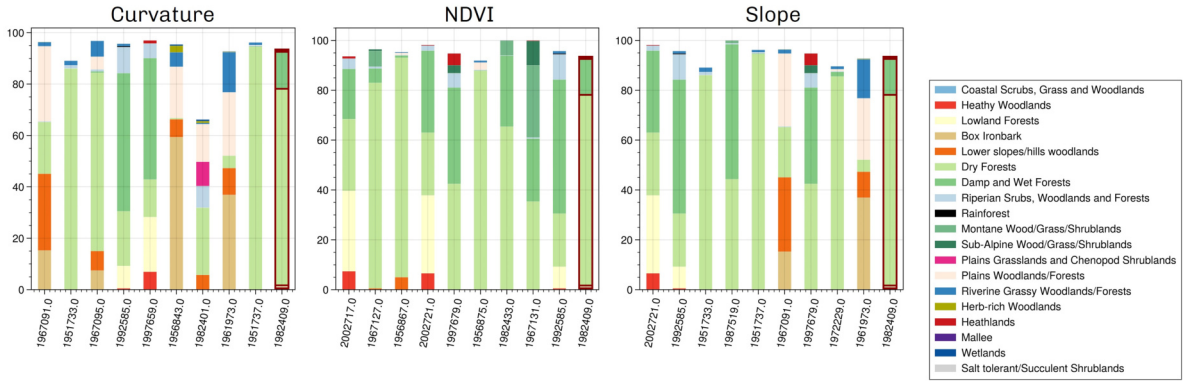

Figure B.4: Comparison of the EVC of the selected control grid points from the three different variables compared to the EVC distribution of the example affected grid point (red box) introduced in B.2

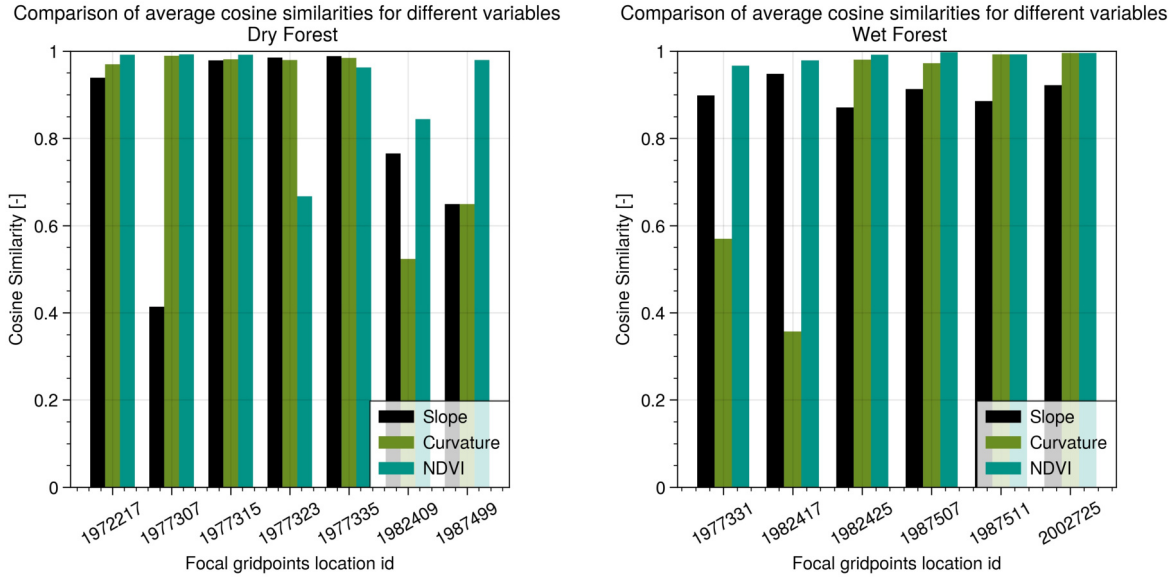

Figure B.5: For each affected grid point, the average cosine similarity with its control grid points is presented. Determined for each variable as control grid points differ per variable

C

Exploration of Burn Scale options

Within this study, a Burn Scale was developed to represent both the severity with which a grid point burned and the percentage affected of that grid point as well. It was deemed necessary to design such a scale due to the coarse spatial scale and consequently the large area that one grid point describes. In developing this burn scale, several options were explored before settling on the Burn Scale as is presented in this study. The different options are presented here. For each scale, the annually averaged slope time series are used to visualise the scale.

The first option was to look solely at the percentage affected of the area the grid point describes. This option is shown in Figure C.1a. The scale distinguishes between different grid points in an intuitive way, but some grid points are presented in the same way due to having almost the same percentage of area affected. However, from Figure 2.7, it became clear that grid points with similar percentages affected may have clearly different fire severity distributions. From the literature, there was an expectation that the fire severity would influence the fire effects as well. To be able to investigate these effects, other options to represent the grid points were explored.

The second option was to use a categorial system in line with other studies such as Bennett et al. (2016), Benyon and Lane (2013), Karna et al. (2020), Lentile et al. (2007), and M. Tanase et al. (2015). After the resampling, for each affected grid point the distribution of the five fire severities was available. These were recategorised into three fire severities: High Fire Severity (FS1 & FS2), Moderate severity (FS3) and Low fire severities (FS4 & FS5). Those three classes were in line with the earlier mentioned studies. The initial class of 'unaffected' remained as it was. Now that the fire severity distribution has been recategorised, for each grid point, it was determined which of these classes had the majority share. The results are shown in Figure C.1b. Some grid points have been classified as unaffected. This is not intuitive as all grid points have been selected on being more than 50% affected. However, this means that of the upper 50%, there is a major part still unaffected. There are no grid points which have a moderate severity as the dominant class, which is unfortunate as this is the critical severity class for tree survival (Benyon & Lane, 2013). Grid points with a dominant moderate fire severity would have been useful in analyzing this criticality. Besides the lack of moderate severity grid points, most grid points are dominantly high severity burned. Using this scale reduces the ability to compare the different grid points based on their burn severity because there is only little variety. Besides that, it is also visually unpleasant if used to represent the time series because it is hard to distinguish the lines. The initial thought as described in Section 2.3.1 that using a categorial scale in line with other studies would not be adequate is therefore confirmed.

The third option was to scale the severity and the percentage affected to capture both. This scale has eventually been chosen for the study. The same re-categorisation as in option two was used to represent High Severity, Moderate Severity, Low Severity and Unaffected. The formula used was as follows:

$$\text{Burn Scale option } 3 = \frac{(\%\,\text{high severity} \times 4) + (\%\,\text{moderate severity} \times 3) + (\%\,\text{low severity} \times 2) + \%\,\text{Unaffected}}{100}$$

where:

- % high severity = fraction fire severity 1 + fire severity 2
- % moderate severity = fraction fire severity 3
- % low severity = fraction fire severity 4 + 5

This scale was designed to include both percentage affected and the fire severity. Using them separately was not adequate, as option 1 ignored the fact that the fire severity should have a substantial effect on the fire impact, and option 2 had too little variety. The idea for this scale was that the area that one grid point describes is so vast, that it is important to describe the percentage of that area affected, but that there also should be a way to incorporate the fire severity in that. The resulting burn scale is shown in Figure C.1c. The interpretation of this scale is such that if the value was 4, the entire grid point was burned by high severity fire, whereas at 1 it was completely unaffected. A value of 2 could both represent a grid point entirely burned by low severity fire, as well as a grid point that is 50% affected by moderate severity fire and 50% unaffected. This makes the physical interpretation of this Burn Scale non-intuitive. The scale is also hard to compare to other studies without assumptions about what high and low Burn Scale values mean. However, the data of this study would be hard to compare to other studies in all cases due to its coarse spatial resolution. Most important was to be able to compare grid points to each other in a way that captured as much information about what happened in the area of the grid point as possible. That is why this Burn Scale option was eventually chosen as the most adequate option.

However, another option was explored as well, which is option 4. This option is based on the fact that Fire Severities 1 to 3 describe both the overstorey and understorey being affected, whereas Fire Severities 4 and 5 describe only understorey disturbance. The ratio between the two could describe how heavily affected the grid points were. The following equation was used to calculate this option:

$$Burn\ Scale\ option\ 4 = \frac{\%\,FS1 + \%\,FS2 + \%\,FS3}{\%\,FS4 + \%\,FS5}$$

This option differentiates between solely understorey burn and disturbance over the entire canopy layer. The reasoning to look at such a scale was that ASCAT measurement would be able to measure overstorey and understorey disturbance simultaneously, whereas NDVI would not react strongly to solely understorey disturbance. The interpretation of the scale is that if the value is 1, there are equal parts FS1—3 and FS4–FS5 burn. If the value is increasingly positive, there is an increasing abundance of overstorey disturbance. If the value is between zero and one, there is a dominant understorey disturbance. The results are shown in Figure C.1d. Most grid points show a value above 1, and only two grid points have a value below zero. Only two grid points would be too little to actually say something about the differences between the behaviours of the different fire severities. Besides that, this scale shows almost no additional information to option 2, but is less intuitive in interpretation. It also does not include the percentage affected. The scale is therefore not more useful than the other scales suggested.

In conclusion, with the coarse resolution of the ASCAT grid points it is hard to find a burn scale that represents the heterogeneity of the fire severity and area of disturbance within that single grid point. The best measure found was Burn Scale 3 which has been used throughout the study. The scale is not as intuitive as options 1 and 2 but contains more necessary information, making it an adequate measure. With this scale, several assumptions had to be made to be able to compare it to other literature, which is unfortunate. For future studies, we advise reiterating the decision for a burn scale for data with such a coarse spatial resolution that inevitably describes a heterogeneous area.

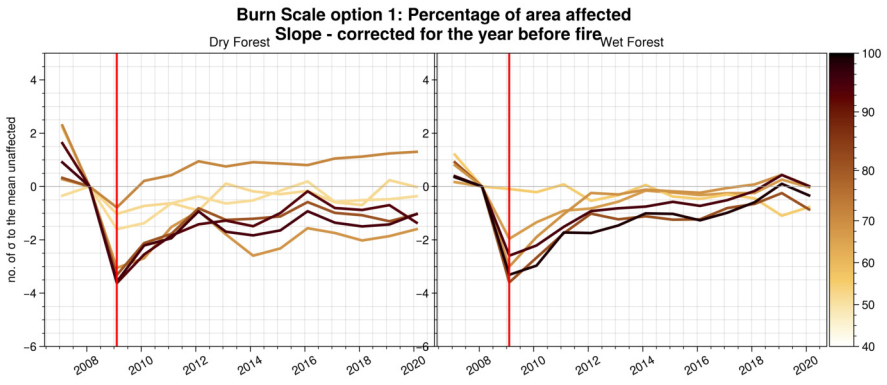

(a) Burn Scale Option 1: Percentage Affected. The percentage affected is determined from the fire severity distributions as shown in 2.7. They are thus based on the Hamming Window resampled fire severities.

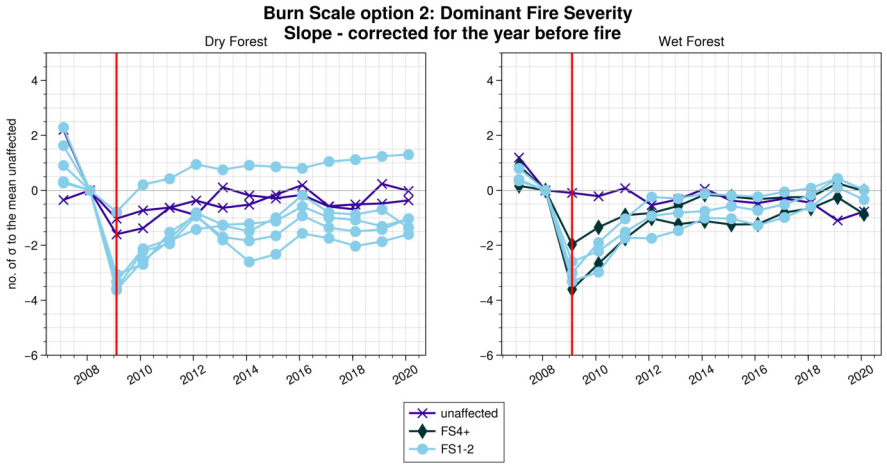

(b) Burn Scale Option 2: Dominant Fire Severity for each grid point. Fire Severity has been re-categorised from the original five-class system to a 3 class system with 'High', 'Moderate' and 'Low' severities. No grid points have the 'Moderate' severity as majority.

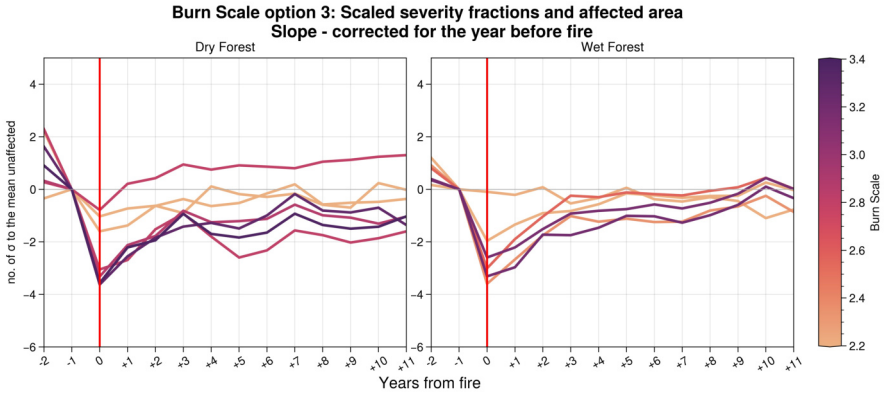

(c) Burn Sccale Option 3: Scaled percentage affected and fire severity to capture the heterogeneity between the grid points. Typically, a higher value is more severely affected and/or more area affected.

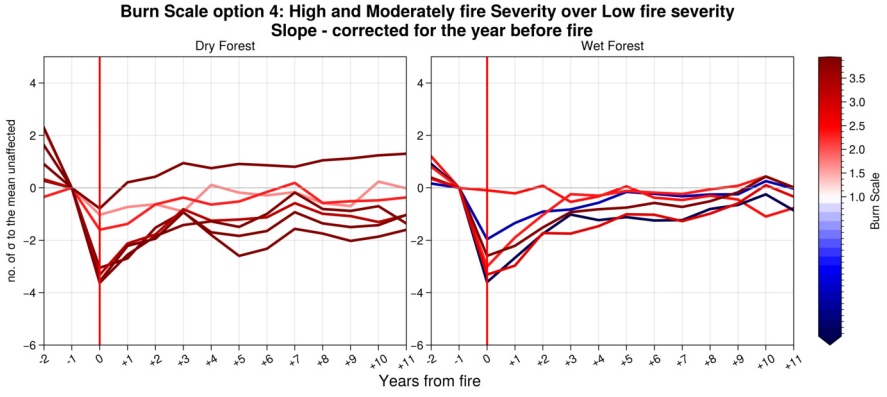

(d) Burn Scale Option 4: Ratio between overstorey affected and understorey affected. A value of one describes an equal ratio between FS1—FS3 and FS4—5. A number above 1 describes more overstorey disturbance, and a value below 1 describes more understorey disturbance.